Ornithology AmericanOrnithology.org

Volume 138, 2021, pp. 1–14
DOI: 10.1093/ornithology/ukaa064

RESEARCH ARTICLE

Latitude does not influence cavity entrance orientation of South American avian excavators

Valeria Ojeda,[1,*] Alejandro Schaaf,[2] Tomás A. Altamirano,[3] Bianca Bonaparte,[4] Laura Bragagnolo,[5] Laura Chazarreta,[6] Kristina Cockle,[3,4] Raphael Dias,[7] Facundo Di Sallo,[4] J. Tomás Ibarra,[8] Silvina Ippi,[9] Adrián Jauregui,[10] Jaime E. Jiménez,[11,12] Martjan Lammertink,[4,13] Fernando López,[14] María Gabriela Núñez Montellano,[15] Martín de la Peña,[16] Luis Rivera,[2] Constanza Vivanco,[2] Miguel Santillán,[17] Gerardo E. Soto,[12] Pablo M. Vergara,[18] Amy Wynia,[19] and Natalia Politi[2]

[1] INIBIOMA (UNComa- CONICET), Bariloche, Río Negro, Argentina
[2] INECOA (UNJujuy-CONICET), Jujuy, Argentina
[3] Department of Forest and Conservation Sciences, University of British Columbia, Vancouver, British Columbia, Canada
[4] IBS (UNMisiones-CONICET), Misiones, Argentina
[5] UNLa Pampa-FCEyN, Santa Rosa, La Pampa, Argentina
[6] Administración de Parques Nacionales (DRPN), Bariloche, Río Negro, Argentina
[7] Centro Universitário de Brasília (UniCEUB), Brasília, Brazil
[8] Center for Local Development (CEDEL) & Center of Applied Ecology and Sustainability (CAPES), Pontificia Universidad Católica de Chile, Villarrica, Chile
[9] Universidad Nacional del Comahue & CONICET (CRUB-UNCo), Bariloche, Río Negro, Argentina
[10] Sección Ornitología, Museo de La Plata, UNLP-CONICET, Buenos Aires, Argentina
[11] Biological Sciences, University of North Texas, Denton, Texas, USA
[12] Universidad de Magallanes & Inst. Ecol. and Bio., Chile
[13] Cornell Lab of Ornithology, Cornell University, Ithaca, New York, USA
[14] INCITAP (UNLPam-CONICET), Santa Rosa, Argentina
[15] IER (UNTucumán-CONICET), Residencia Universitaria Horco Molle, Tucumán, Argentina
[16] Tres de Febrero 1870, (3080) Esperanza, Santa Fe, Argentina
[17] Museo de Historia Natural de La Pampa, La Pampa, Argentina
[18] Dto. de Gestión Agraria, Universidad de Santiago de Chile, Santiago, Chile
[19] Department of Biological Sciences and Advanced Environmental Research Institute, University of North Texas, Denton, Texas, USA
[*] Corresponding author: valeriaojeda@comahue-conicet.gob.ar

Submission Date: July 22, 2019; Editorial Acceptance Date: August 12, 2020; Published January 7, 2021

ABSTRACT

In the Northern Hemisphere, several avian cavity excavators (e.g., woodpeckers) orient their cavities increasingly toward the equator as latitude increases (i.e. farther north), and it is proposed that they do so to take advantage of incident solar radiation at their nests. If latitude is a key driver of cavity orientations globally, this pattern should extend to the Southern Hemisphere. Here, we test the prediction that cavities are oriented increasingly northward at higher (i.e. colder) latitudes in the Southern Hemisphere and describe the preferred entrance direction(s) of 1,501 cavities excavated by 25 avian species (n = 22 Picidae, 2 Trogonidae, 1 Furnariidae) across 12 terrestrial ecoregions (15°S to 55°S) in South America. We used Bayesian projected normal mixed-effects models for circular data to examine the influence of latitude, and potential confounding factors, on cavity orientation. Also, a probability model-selection procedure was used to simultaneously examine multiple orientation hypotheses in each ecoregion to explore underlying cavity-orientation patterns. Contrary to predictions, and patterns from the Northern Hemisphere, birds did not orient their cavities more toward the equator with increasing latitude, suggesting that latitude may not be an important underlying selective force shaping excavation behavior in South America. Moreover, unimodal cavity-entrance orientations were not frequent among the ecoregions analyzed (only in 4 ecoregions), whereas bimodal (in 5 ecoregions) or uniform (in 3 ecoregions) orientations were also present, although many of these patterns were not very clear. Our results highlight the need to include data from under-studied biotas and regions to improve inferences at macroecological scales. Furthermore, we suggest a re-analysis of Northern Hemisphere cavity orientation patterns using a multi-model approach, and a more comprehensive assessment of the role of environmental factors as drivers of cavity orientation at different spatial scales in both hemispheres.

Keywords: excavation behavior, latitudinal gradient, Neotropical birds, oceanic influence, selective orientation, Southern Hemisphere, thermal advantage

LAY SUMMARY

- We tested the hypothesis that avian excavators (e.g., woodpeckers) increasingly orient their cavities toward the equator (sun) as latitude increases (i.e. colder climate), between 15°S and 55°S in the Southern Hemisphere.
- We found no evidence that latitude influenced orientation.
- The preferred entrance direction(s) of 1,501 cavities excavated by 25 South American avian excavators from 12 ecoregions (bioclimatic areas) were bimodal (5 ecoregions), followed by unimodal (4 ecoregions), and uniform (3 ecoregions).
- The patterns of cavity orientation at the ecoregions considered, and the lack of relationship with latitude differed strikingly from previous studies from the Northern Hemisphere, which highlights the importance of using multi-model analytical approaches for circular data, as well as the need to include understudied biotas to improve inferences in macroecology.

La latitud no influye en la orientación de la entrada de las cavidades excavadas por aves de Sudamérica

RESUMEN

En el Hemisferio Norte, muchos excavadores de cavidades arbóreas (e.g., pájaros carpinteros) orientan la entrada de sus cavidades hacia el ecuador, a medida que la latitud aumenta. Esto se debería a una ventaja térmica de la radiación solar ingresando al nido, en climas más fríos. Si la latitud tiene un rol determinante en las orientaciones de las cavidades excavadas a nivel global, un patrón similar (pero contrario) se debería evidenciar en el Hemisferio Sur. Nuestros objetivos fueron probar la predicción que, en el Hemisferio Sur, las cavidades orientan crecientemente al norte al aumentar la latitud, y describir la(s) preferencia(s) de orientación en una muestra de 1,501 cavidades excavadas por 25 especies (n = 22 Picidae, 2 Trogonidae, 1 Furnariidae) en 12 ecorregiones (15°S–55°S) de Sudamérica. Evaluamos la influencia de la latitud sobre la orientación (y de otros factores potencialmente influyentes) en base a modelos bayesianos mixtos para datos circulares con distribución normal proyectada, y exploramos los patrones de orientación subyacentes en cada ecorregión mediante un análisis multi-modelo, comparando varias estructuras circulares simultáneamente. Contrariamente a nuestras predicciones en base a los patrones del Hemisferio Norte, las aves de Sudamérica no tendieron a orientar sus cavidades hacia el norte al incrementar la latitud, lo que sugiere que la latitud tiene baja influencia en el comportamiento de excavación de las aves sudamericanas. De hecho, las orientaciones unimodales no fueron frecuentes (cuatro ecorregiones), siendo también comunes las bimodales (cinco ecorregiones) y uniformes (tres ecorregiones), aunque varios de estos patrones de orientación fueron poco netos. Nuestros resultados desatacan la importancia de incluir datos de biotas y regiones poco estudiadas para lograr buenas inferencias en macroecología. Además, sugerimos re-analizar, bajo una mirada de modelos múltiples, los patrones de orientación en el Hemisferio Norte, y en ambos hemisferios, evaluar más exhaustivamente el rol de factores ambientales alternativos como promotores de orientaciones de cavidades, en diferentes escalas espaciales.

Palabras clave: aves neotropicales, comportamiento de excavación, gradiente latitudinal, Hemisferio Sur, influencia oceánica, orientación selectiva, ventaja térmica

INTRODUCTION

Avian excavators such as woodpeckers (Picidae) create nesting and roosting cavities in trees and alternative substrates (e.g., cacti, wooden posts, termitaria, and river banks). A well-documented pattern among excavated cavities is that they often occur in non-random orientations (e.g., Lawrence 1967, Conner 1975, Inouye et al. 1981, Zwartjes and Nordell 1998). Multiple explanations have been proposed for non-random cavity orientation in birds, including social factors (e.g., communication, Mennill and Ratcliffe 2004), predation risk and competition (Albano 1992), substrate properties (leaning or branching, Zwartjes and Nordell 1998), directional bias in dispersal/colonization of heart-rot fungi (Losin et al. 2006), and optimization of cavity microclimate to increase nestling development, reduce parental energy investment, and/or improve fledging success (Lawrence 1967, Inouye et al. 1981, Korol and Hutto 1984, Hansell 2000, Deeming 2002, Mezquida 2004, Dawson et al. 2005, Mainwaring et al. 2017). Whereas most of these factors operate at a local or regional scale, climate (e.g., wind, rainfall, and solar radiation) may also predict large-scale macroecological patterns.

Direct evidence of the effect of solar radiation on cavity microclimate has been observed in multiple studies at north temperate latitudes, where cavities facing the equator (i.e. south) are significantly warmer than those facing away from the equator (i.e. north; Derby and Gates 1966, Wiebe 2001, Ardia et al. 2006, Butler et al. 2009). Landler et al. (2014) conducted a meta-analysis of cavity entrance orientation from 80 populations of 23 woodpecker species across 35 degrees of latitude (25°N–60°N) in the Northern Hemisphere and concluded that temperature, as determined by latitude and continental effects, was the major driver of orientation. These authors found that cavity entrance orientation was non-random in 39% of the studies analyzed and that, independent of taxonomic relationships, woodpecker populations occurring at higher latitudes (i.e.

facing higher risks of hypothermia) orient their cavities more toward the equator to take advantage of incident solar radiation in their nests. These patterns were stronger for North American than Eurasian populations at similar latitudes. Because the focus of the work of Landler et al. (2014) was restricted to an examination of the effect of latitude and continent on the mean direction of woodpecker cavity orientation, these authors based their exploration of the angular deviations from random (i.e. uniform) distribution using a Rayleigh test, which has low power to reject the null hypothesis of uniformity when more than one mode is present (Landler et al. 2019). Other patterns beyond unimodality (i.e. bi- or multimodal patterns, Korol and Hutto 1984, Dobkin et al. 1995, Butcher et al. 2002, Rico and Sandoval 2014), which may relate to cavity thermal efficiency, were not explored in the Landler et al. (2014) study. Extreme seasonal conditions (e.g., cold winters or hot summers) and trade-offs between local climatic drivers (e.g., wind/rainfall vs. solar incidence) may result in complex scenarios for the optimization of cavity microclimate by excavators in any ecoregion. Hence, analyzing non-unimodal cavity orientations may also provide insight on factors that likely influence cavity thermal properties among excavator populations.

Understanding the factors driving orientation of avian cavities on a global scale should include examining latitudinal effects in under-represented regions (Landler et al. 2014). A current challenge is to test whether these large-scale patterns in orientation associated with the Northern Hemisphere also occur in the Southern Hemisphere. The "solar radiation advantage" hypothesis predicts that birds at low southern latitudes (i.e. warmer locations) will orient their cavities south (away from the sun) to avoid over-heating, as long as the angles of incidence of solar radiation are sufficient to exert an effect on cavity microclimate (i.e. not too close to the equator). Conversely, at the highest southern latitudes (i.e. colder extremes), cavities should orient northwards toward the sun to reduce energy investment in thermoregulation. This macroecological orientation pattern implicitly requires that unimodal woodpecker cavity entrance orientations be commonplace in the latitudinal extremes of the Southern Hemisphere. Between the extremes of southern latitudes, one might expect both a preferred orientation, or a uniform distribution depending upon which factors are most important.

Macroecological factors that may conceal or dilute the effect of solar radiation should be considered in cavity orientation vs. latitudinal gradient studies at continental scales, whenever possible. Among those with great potential to affect cavity thermal properties, and adaptive responses by excavator species (i.e. orientation patterns), are elevation (McCaffrey and Galen 2011), continent-scale climate (Landler et al. 2014), and ecoregion (Nado and Kaňuch 2017). The extent to which local climate is influenced by sea-landmass interactions at the continental scale can be translated into inland thermal severity, with annual (and daily) temperature ranges increasing as the moderating influence of water disappears (McBoyle and Steiner 1972, Mikolaskova 2009). In turn, ecoregions, representing distinct biotas and nested within biomes and realms, provide a framework for comparisons among units and the identification of representative climate, habitats, ecological phenomena, and species assemblages (Olson et al. 2001). An additional factor influencing cavity orientation is the body size of avian excavators. The regulation of body temperature and water loss in birds are size-dependent (Prinzinger et al. 1991); therefore, response mechanisms to hyper- or hypothermic conditions are likely to vary with body size.

Here we investigate the trends in entrance orientation of excavated cavities across a range of tropical to subpolar habitats in South America. Using data from multiple study systems, we: 1) test the "southern predictions" for the hypothesis that latitude—and its associated solar radiation and ambient temperature—are dominant drivers of cavity orientation at continental scales, while we explore further macroecological variables (e.g., elevation, ecoregion) with potential effects on cavity orientation; and (2) describe the preferred direction(s) of cavity entrances from excavator communities in 12 South American ecoregions. We include circular trends beyond unimodality to describe patterns of cavity orientation at all latitudes to enrich our understanding of cavity construction behavior by birds at a global scale.

MATERIALS AND METHODS

Study Area

The present study combines data on excavated cavities from short- and long-term field studies of avian cavity excavators and their nest and roost sites collected in Argentina, Brazil, and Chile (Tables 1 and 2, Figure 1). Our data were obtained at 21 field sites that correspond to 12 South American ecoregions, as defined by Olson et al. (2001). Because of different methodologies, the parallelism among data sets, sites, and ecoregions was not always straightforward (see Supplementary Material Appendix S1 for details).

Close to the equator, the angles of incidence of solar radiation on vertical objects are near zero (i.e. little incidence, Idowu et al. 2013). Hence, to enable potential effects of the sun on cavities excavated into vertical tree trunks, minimum latitude was tentatively established at 15°S, areas considered among the warmest (i.e. ecuatorian) climates on Earth (Kottek et al. 2006). The maximum latitude was

TABLE 1. Orientation of 1,501 excavated cavities distributed across 12 ecoregions of southern South America (country initials in parentheses: AR = Argentina, BR = Brazil, CH = Chile). Mean temperatures (*T*) were obtained for each ecoregion from Climate-Data Org. (https://en.climate-data.org) for closest or midpoint cities, where A = annual, S = summer (warmest month), and W = winter (coldest month). Cavity orientation patterns were summarized from the model selection procedure given in Supplementary Material Appendix S3. The orientation pattern according to the top model (i.e. lowest ΔAIC_c, highest w_i) is shown for each ecoregion. Alternative orientations are also shown whenever the ratio between ΔAIC_c w_i values of the top and following model(s) <2.5 (i.e. the strength of evidence in favor of the top-model was low, compared to the other models; see Symonds and Moussalli 2011); the similarly supported orientations are in italic. Orientation patterns whose ΔAIC_c $w_i > 0.7$ (considered almost unequivocal) are in bold.

Ecoregion (North to South)		Mean location (m.a.s.l.)	Mean *T* (°C)	Cavities (*n*)	Cavity orientation patterns (ΔAIC_c w_i)
1.	Cerrado (BR)	15.90°S 47.90°W (1060)	A: 21.1 S: 22.3 W: 18.9	50	**Uniform (0.70)**
2.	Dry Chaco (AR)	23.65°S 65.27°W (400)	A: 22.2 S: 27.1 W: 15.8	46	Bimodal axial NE—SW (0.60)
3.	Southern Andean Yungas (AR)	23.90°S 64.90°W (720)	A: 21.0 S: 25.9 W: 14.5	186	Unimodal W (0.61)
4.	Atlantic Forest (AR)	26.61°S 54.12°W (530)	A: 18.5 S: 23.2 W: 13.6	113	*Bimodal axial NW—SE (0.42)* *Uniform (0.38)*
5.	High Monte (AR)	26.07°S 65.68°W (1695)	A: 16.2 S: 21.1 W: 9.9	40	**Unimodal W (0.84)**
6.	Humid Chaco (AR)	26.80°S 59.60°W (50)	A: 21.4 S: 27.2 W: 15.2	46	**Uniform (0.84)**
7.	Parana Flooded Savanna (AR)	30.62°S 59.95°W (40)	A: 20.0 S: 26.2 W: 14.0	9	*Uniform (0.49)* *Unimodal NW (0.47)*
8.	Northern Espinal (AR)	31.47°S 60.92°W (40)	A: 18.9 S: 25.8 W: 12.4	78	Unimodal N (0.55)
9.	Humid Pampas (AR)	35.31°S 57.21°W (10)	A: 16.0 S: 22.7 W: 10.2	77	Bimodal axial S—N (0.60)
10.	Southern Espinal (AR)	36.91°S 64.28°W (140)	A: 15.3 S: 23.4 W: 7.7	52	*Unimodal ESE (0.345)* *Bimodal non-axial SSW—NE (0.342)* *Uniform (0.18)*
11.	Valdivian Temperate Rain Forests (CH, AR)	40.17°S 71.78°W (950)	A: 9.8 S: 15.8 W: 4.3	638	*Bimodal non-axial NNE—S (0.38)* *Bimodal axial N-S (0.24)* *Unimodal E (0.22)* *Uniform (0.16)*
12.	Magellanic Subpolar Forests (CH)	54.95°S 67.66°W (60)	A: 5.6 S: 9.3 W: 1.8	166	**Bimodal non-axial NW—SE (0.92)**

55°S, at the southern tip of South America. These extremes created a latitudinal range of ~40° for comparison, with a longitudinal range of 47°W–72°W, and from sea level to ~1,700 m in elevation.

Field Methods

We included data collected by a variety of methods (e.g., cavity surveys, nest searching, and radio-telemetry) that we considered unbiased in terms of cavity orientation. We included avian-excavated cavities in substrates where all orientations were available (i.e. trees, posts, and free-standing termitaria), and excluded cavities in directional substrates (earth banks or termitaria attached to trees). Non-excavated cavities, although occasionally used by excavators, were excluded from our datasets. We identified the excavator species of most cavities, either by direct observation or by inferring from differences in sizes and shapes of cavity entrance, based upon investigator experience.

TABLE 2. Information on the South American excavator species in this study. Species with the minimum sample size (≥9 cavities) included in the Bayesian models are in bold. Avian taxonomy and nomenclature follow the South American Classification Committee (Remsen et al. 2020).

Species	Cavities (*n*)		Mean weight (g)	Ecoregions with cavities (sensu Olson et al. 2001)
	<9	≥9		
Woodpeckers (Picidae)				
Picumnus cirratus	–	97	9.5	Dry Chaco/Humid Chaco/Northern Espinal/Parana Flooded Savanna/Southern Andean Yungas
Picumnus temminckii	–	10	11.2	Atlantic Forests
Melanerpes flavifrons	–	10	56.5	Atlantic Forests
Melanerpes cactorum	–	60	41.0	High Monte/Northern Espinal/Humid Chaco
Melanerpes candidus	4	–	117.0	Humid Chaco/Northern Espinal
Veniliornis mixtus	–	11	33.4	Southern Espinal/Humid Chaco/Northern Espinal/Parana Flooded Savanna
Veniliornis lignarius	–	73	37.0	Valdivian Temperate Rain Forests
Veniliornis passerinus	2	–	30.5	Parana Flooded Savanna
Veniliornis frontalis	1	–	35.0	Southern Andean Yungas
Veniliornis spilogaster	2	–	40.0	Atlantic Forests
Campephilus leucopogon	–	126	242.0	Dry Chaco/Humid Chaco/Northern Espinal/Southern Andean Yungas
Campephilus magellanicus	–	539	337.5	Valdivian Temperate Rain Forests/Magellanic Subpolar forests
Campephilus robustus	6	–	269.0	Atlantic Forests
Campephilus melanoleucos	2	–	232.5	Cerrado
Dryocopus lineatus	–	15	211.0	Atlantic Forests/Cerrado
Dryocopus schulzi	2	–	No data	Humid Chaco
Celeus galeatus	–	9	131.0	Atlantic Forests
Celeus lugubris	1	–	14.5	Humid Chaco
Colaptes melanochloros	–	128	115.0	Humid Chaco/Atlantic Forests/Humid Pampas/High Monte/Northern Espinal/Parana Flooded Savanna
Colaptes campestris	–	113	168.5	Atlantic Forests/Cerrado/Humid Pampas/Northern Espinal/Parana Flooded Savanna
Colaptes pitius	–	27	131.5	Valdivian Temperate Rain Forests
Colaptes rubiginosus	1	–	70.0	Southern Andean Yungas
Trogons (Trogonidae)				
Trogon surrucura	–	14	67.1	Atlantic Forests
Trogon rufus	4	–	52.5	Atlantic Forests
Ovenbirds (Furnariidae)				
Pygarrhichas albogularis	–	152	23.5	Valdivian Temperate Rain Forests
TOTAL	25	1,384		

We measured the cardinal orientations of the excavated cavities in degrees, with different compass models (either global or balanced for the Southern Hemisphere), without magnetic declination correction. We used hand-held GPS devices set at WGS84 to obtain the geographic coordinates (in degrees) of each cavity. Elevation (meters above sea level [m.a.s.l.]) was obtained using the same GPS devices, topographic maps, or Google Earth. Mean weights for the excavator species, a surrogate for body size, were obtained from del Hoyo et al. (2018).

Data Processing and Analyses

We corrected cavity orientation considering the magnetic declination (as per Evans 2017). We examined the effects of latitude on cavity orientations with Bayesian projected normal mixed-effects models that allowed the analysis of a circular variable such as cavity orientation. The main purpose of these models was to combine an explicit hypothesis test (i.e. test for the importance of latitude in driving cavity orientation) with exploratory analyses on additional variables with potential effects on the orientation patterns. All statistical analyses were performed in R, PAUP* 4.0.0. (R Core Team 2020).

We investigated collinearity using pairwise correlations between the explanatory variables considered (Zuur et al. 2009, Dormann et al. 2013). If two variables correlated at ≥0.6, one was eliminated from further analyses. Therefore, longitude was not included in analyses because of its high correlation with latitude (Pearson's r = 0.6). After this variable selection process, we built a full model using the package *bpnreg* for circular data (Cremers 2018, Cremers and Klugkist 2018) (codes in Supplementary Material Appendix S2). We chose a non-informative prior

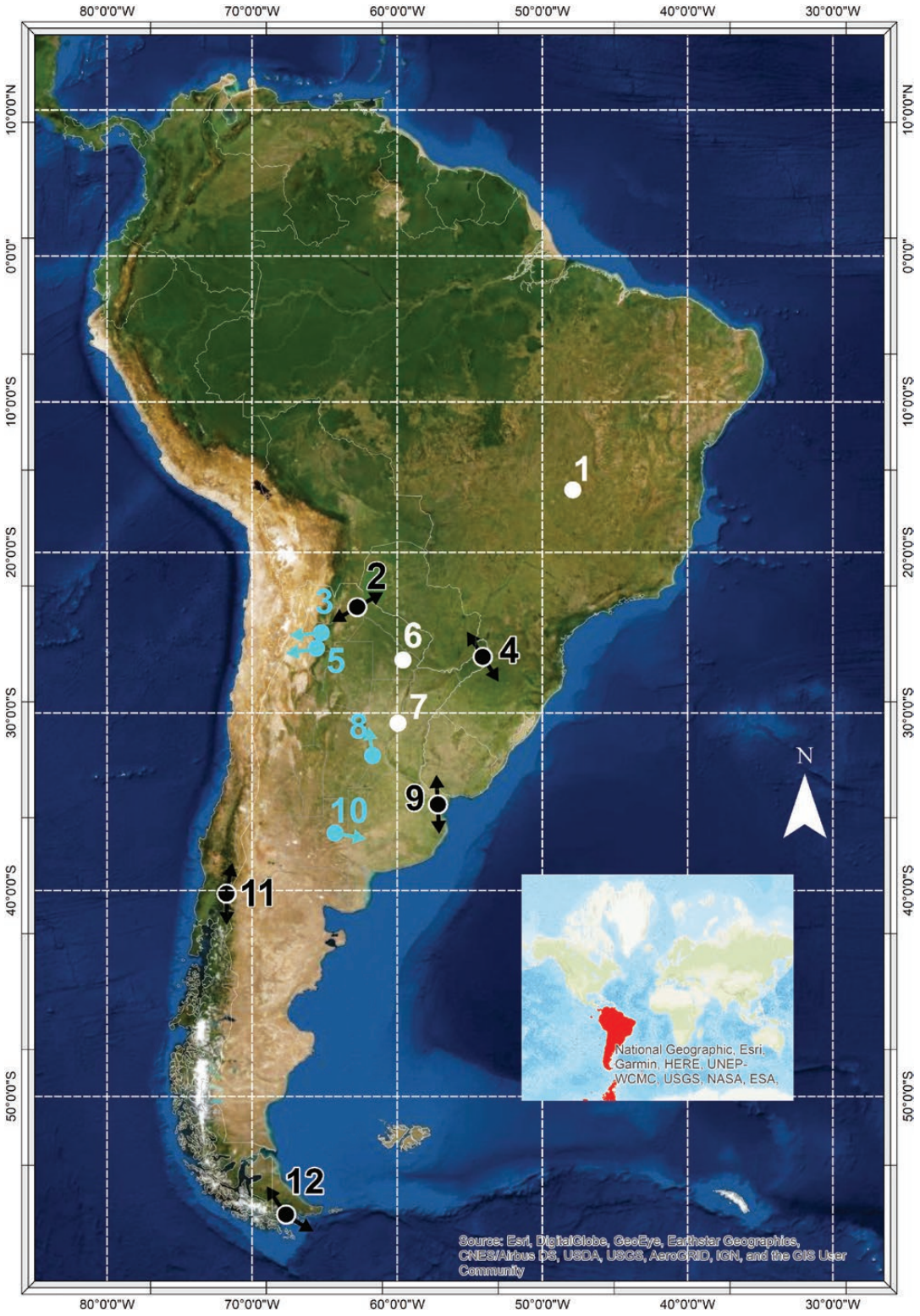

FIGURE 1. Satellite image displaying the geographic distribution of studies of avian cavity excavators and their nest and roost sites in 12 ecoregions of South America, arranged southwards from ~15°S to ~55°S. Ecoregion names are provided in Table 1. Cavity orientation patterns correspond to the top model (i.e. lowest ΔAIC_c) in the multi-model selection procedure applied (see Supplementary Material Appendix S3) and are summarized by symbols: white indicates uniform distributions, light blue indicates unimodal (one arrow) orientations, and black indicates bimodal (two arrows) distributions.

distribution for the parameters. In the full model we included latitude, elevation, and species mean weight as explanatory variables. Paired interactions between latitude and the other two explanatory variables were also considered. From this full model, we generated 10 different mixed-effects models (including the intercept-only model) where latitude was kept fixed, as recommended by Grueber et al. (2011) when there is a particular factor of interest (a "focal parameter"). These models were ranked by the Watanabe-Akaike information criterion (WAIC), which is suitable for selection of Bayesian hierarchical models (Watanabe 2010, Gelman et al. 2014, Link and Sauer 2016, Cremers and Klugkist 2018). The WAIC interpretation is analogous to that of the Akaike Information Criterion (AIC, Akaike 1973), where lower values indicate stronger support. We followed Burnham and Anderson (2004) and Burnham et al. (2011), considering models with a difference relative to the best model ΔAIC (or ΔWAIC) ≤ 2 to have substantial support, models with ΔAIC (or ΔWAIC) between 2 and ≤7 to have considerably less support (but should rarely be dismissed), and models with ΔAIC (or ΔWAIC) > 7 to have little or no support. Ecoregion and excavator species were included as random effects. But as the *bpnreg* package only allows one random effect at a time, we built two full models as previously explained, one with ecoregion and one with the avian excavator species, as the random effect, to select the best random structure. We compared these two models with different random structure using the WAIC.

For the 3 continuous explanatory variables, we calculated the 3 circular coefficients that describe the relationship between the circular variable (i.e. cavity entrance orientation) and the predictor (e.g., latitude), because the slope of this line (i.e. the effect of x) varies across values of x. The first coefficient, b_c, represented the slope of the circular regression line at the inflection point; the second coefficient, SAM, represented the slope of the circular regression line at the mean of the predictor, and the third coefficient, AS, represented the mean slope over all values of x (Cremers and Klugkist 2018, Cremers et al. 2018). Finally, for the model with the lowest WAIC, we calculated the posterior mean and the highest posterior density interval (HPD) of the circular coefficients, which was the smallest interval that included 95% of the posterior distribution. For each model simulation, Markov chain Monte Carlo (MCMC) was run for 10,000 iterations, with a 1,000-iteration burn. We assessed convergence of the MCMC chain for all parameters in the full model using a traceplot (Cremers and Klugkist 2018).

Our description of the preferred direction(s) of cavity entrances from excavator communities in different ecoregions was based on a probability model selection procedure developed to simultaneously examine multiple orientation hypotheses (Schnute and Groot 1992), implemented by Fitak and Johnsen (2017) into the R package *CircMLE* (PAUP* 0.2.3., codes in Supplementary Material, Appendix S2), which in turn required the *Circular* package (Lund and Agostinelli 2017). Even weakly oriented datasets may be detected using the approach in *CircMLE* (Fitak and Johnsen 2017). For a given data set, *CircMLE* calculates the maximum likelihood of several alternative models of cavity entrance orientation; the circular distributions evaluated in this study included uniform, unimodal, and bimodal (axial and non-axial) models (details in Supplementary Material, Appendix S3). These models were compared using AIC_c for small sample sizes (Hurvich and Tsai 1989, Burnham and Anderson 2004), following the guidelines previously given for the Bayesian models. We further used the Akaike weight (w_i), the probability that a particular model was the best (approximating) model given the experimental data and the collection of models considered. The ratio of the weight of model i vs. weight of model j quantified the strength of evidence in favor of model i over model j, whenever more than one model was retained based on the ΔAIC_c (Burnham et al. 2011, Portet 2020).

Although rejection of non-uniformity may fail in situations where the possible number of modes is >2 (i.e. multimodal data, which is not considered in the *CircMLE*), graphic analyses of the data allowed detecting patterns of concentrations around >2 different modes. Regardless, multimodal situations that do not visually differ from uniform, unimodal, or bimodal distributions may not be very ecologically important.

RESULTS

We found 1,501 cavities, of which 1,409 could be assigned to one of 25 avian species (Table 2). All species but one (Lineated Woodpecker [*Dryocopus lineatus*]) were endemic to South America, and they varied in size from the White-barred Piculet (*Picumnus cirratus*, ~10 g) to the Magellanic Woodpecker (*Campephilus magellanicus*, ~340 g). Most cavities belonged to large-sized (>200 g, n = 688), followed by small-sized (<100 g, n = 438) and mid-sized (100–200 g, n = 281) species. Fifteen excavator species had sufficient sample sizes (≥9 cavities) to be considered in the Bayesian models (Table 2). Cavities (n = 25) of the other 10 species, along with 92 cavities that could not be assigned to a species (Supplementary Material Appendix S1), were used only for exploring the underlying angular cavity distribution at each ecoregion.

Our analyses based on the Bayesian projected normal mixed-effects models suggest that latitude, elevation, and mean weight of excavator species were poor predictors of cavity entrance orientation. Models with ecoregion (WAIC = 5080.08) and with excavator species

(WAIC = 5081.23) as the random factor were similarly supported. However, for simplicity, we present the results from the model with the lowest WAIC here (Tables 3 and 4), while results from the other model sets are presented as Supplementary Material Appendix S4. All models with ecoregion as the random variable had ΔWAIC ≤7, and included the intercept-only model, suggesting that none of the variables included in these models was useful in explaining the variability in the cavity entrance orientation. The lowest WAIC model differed by only 0.84 WAIC from the null model, and included latitude, elevation, species mean weight, and two interactions: latitude and elevation, and latitude and species mean weight, as explanatory variables. For this model, the posterior mean of the intercept variance on the circle was estimated at 0.75, and its HPD interval was 0.40–0.99. The HPD intervals for the 3 circular coefficients (bc, SAM, and AS) for latitude and the other variables in this model included zero (Table 4). Thus, we did not find evidence that any of the variables in the top model influenced cavity entrance orientation at the inflection point, at mean latitude, elevation or species weight, or on average across latitudes, elevations, and species weights.

Results for the Bayesian circular models constructed with excavator species as the random factor were similar to the results just presented for ecoregion as the random factor (Supplementary Material Appendix S4), with the null model included among those with ΔWAIC < 7. Moreover, the estimated parameters for the variables included in the top model were similar to those of the top model with ecoregion as the random factor, where the HPD intervals always included zero.

Based on our evaluation of cavity entrances from excavator communities using the approach in *CircMLE*, the best approximating model (i.e. top model, with lowest AIC_c) corresponded to uniform orientations in three ecoregions, unimodal orientations in four ecoregions, and bimodal orientations in the remaining 5 ecoregions, with 3 axial and 2 non-axial top distributions (Supplementary Material Appendix S3, Table 1, Figure 1). In 4 ecoregions (in italic in Table 1), the ratio between w_i values of the top and following model was <2.5, which means that the top model was not much better than the next best model (AIC_c w_i values are shown in Supplementary Material Appendix S3). This entails uncertainty regarding the circular distribution of the data, as the alternatives lead to very different orientation patterns (see Symonds and Moussalli 2011). In contrast, 4 ecoregions (in bold in Table 1) showed rather unequivocal orientation patterns (i.e. top model AIC_c w_i > 0.7), meaning that there is at least a 70% chance that it truly is the best approximating model describing the data given the candidate set of orientations considered. Between these extremes, the strength of evidence in favor of the top model was reasonably high (i.e. the ratio between ΔAICc w_i of the top and following model(s) >2.5) in 4 other ecoregions, such that a single most probable model (2 bimodal and 2 unimodal orientation patterns) can be defined.

Graphical analyses of the distributional histograms in Supplementary Material Appendix S3 do not provide evidence of tight concentrations around >2different modes (i.e. multimodality). Interestingly, directional data voids (i.e. potential avoidance of certain orientation ranges), which will not be detected by analytical tools (including our multi-model approach), appear to occur at least in the Magellanic Subpolar Forests (fewer SW-oriented cavities than those in all other directional twelfths), and the Southern Espinal (zero NW-oriented cavities).

DISCUSSION

Southern Predictions for the "Solar Radiation Advantage" Hypothesis

We found no evidence to support the hypothesis that birds orient their cavities more toward the equator with increasing latitude—or away from sun incidence at low latitudes—in the Southern Hemisphere. Our result contrasts

TABLE 3. Bayesian projected normal circular mixed-effects models that test for the effects of latitude, elevation, species mean weight, and the interactions between latitude and the other two explanatory variables on cavity orientation of South American avian excavators where ecoregion is a random factor. Models are ordered from lowest to highest Watanabe-Akaike information criterion (WAIC, Watanabe 2010). The log pointwise predictive density (*lppd*, the log-likelihood evaluated at the posterior simulations of the parameter values) and the effective number of parameters (*pD*, a measure of model complexity computed according to Gelman et al. 2014) are provided (Hooten and Hobbs 2015, Vehtari et al. 2017).

Model	*lppd*	*pD*	WAIC	ΔWAIC
Latitude + Elevation + Weight + Latitude * Elevation + Latitude * Weight	−2520.14	18.79	5077.85	0.00
Latitude + Weight + Latitude * Weight	−2528.68	10.26	5077.88	0.03
Latitude + Elevation + Weight + Latitude * Weight	−2525.67	13.51	5078.36	0.51
Null model	−2528.19	2.00	5078.69	0.84
Latitude + Elevation	−2526.11	13.88	5079.99	2.14
Latitude + Elevation + Weight + Latitude * Elevation	−2520.53	19.76	5080.59	2.74
Latitude	−2530.01	10.51	5081.03	3.18
Latitude + Elevation + Latitude * Elevation	−2525.48	15.30	5081.57	3.72
Latitude + Elevation + Weight	−2523.13	18.16	5082.58	4.73
Latitude + Weight	−2529.05	12.84	5083.77	5.92

TABLE 4. Posterior modes of the circular regression coefficients for the variables included in the lowest WAIC model (see Table 3), where b_c is the slope of the circular regression line at the inflection point, SAM is the slope of the circular regression line at the average of the predictor, and AS is the average slope over all values of the each predictor variable. LB HPD and UB HPD indicate the lowest and the upper bounds of the highest posterior density interval of the coefficients, respectively (Cremers and Klugkist 2018).

		Mode	LB HPD	UB HPD
Latitude	b_c	5.73	−277.25	201.31
	SAM	2.62	−56.21	86.04
	AS	−6.25	−81.48	82.73
Elevation	b_c	−0.06	−3.29	3.40
	SAM	−0.05	−1.37	1.06
	AS	−0.05	−0.80	0.37
Species mean weight	b_c	0.16	−22.99	22.05
	SAM	0.17	−4.85	5.77
	AS	0.13	−6.06	5.64
Latitude * Elevation	b_c	−0.006	−0.68	0.50
	SAM	−0.003	−0.21	0.20
	AS	0.003	−0.08	0.11
Latitude * Species mean weight	b_c	−0.03	−1.86	1.74
	SAM	−0.02	−0.81	0.84
	AS	−0.02	−1.15	1.47

with the "global" pattern shown by Landler et al. (2014) for the Northern Hemisphere, whereby more northerly cavities were more often oriented toward the south. Although the additional macroecological factors assessed in our Bayesian models frequently influence nest orientation in birds in other studies (Zwartjes and Nordell 1998, Hansell 2000, Deeming 2002, Burton 2006, 2007, Mainwaring et al. 2017), they were not good predictors of cavity orientation in South America. Elevation was a promising candidate co-driver of cavity orientation, as many animals exhibit microhabitat adjustments in response to elevation (e.g., Carey 1980, Zerba and Morton 1983, Walsberg 1985, Carothers et al. 1998, McCaffrey and Galen 2011), but it did not affect cavity orientations in our study.

Unexpectedly, cavity entrances were not oriented unimodally at our latitudinal extremes. Our northernmost study, in the tropical Cerrado, was more than 10° closer to the equator than the southernmost study (i.e. Zwartjes and Nordell 1998) analyzed by Landler et al. (2014). We had predicted that this site would exhibit an avoidance of solar radiation. Instead, cavity entrances aligned uniformly, with high model support (top model AIC_c w_i = 0.7, Supplementary Material Appendix S3). In turn, cavities located at the southernmost site (Magellanic Subpolar Forests) oriented strongly bimodally, a pattern with the highest support (top model AICc w_i > 0.9, Supplementary Material Appendix S3). Only two other ecoregions had strongly supported orientation patterns of cavity entrances: the Humid Chaco (uniform), and the High Monte (unimodal). Hence, departing from patterns described for the Northern Hemisphere (as per Landler et al. 2014), unimodal orientation of cavity entrance was rare among South American avian excavators.

The poor support for latitude as a driver of cavity entrance alignment in our study may be explained, totally or in part, by continental effects, as proposed by Landler et al. (2014) for excavators in the Northern Hemisphere. In South America, the relationship between land mass and latitude is inverse to that of Palearctic and Nearctic regions, and hence, oceanic influence increases with latitude (Berman et al. 2012). In the Southern Hemisphere, seasonal cycles revolve around the presence and absence of precipitation and prevailing winds, rather than major swings in temperature that characterize seasonality in the Northern Hemisphere (Stevens 2012); an exception occurs at the narrow forest strip east of the Andes of north Patagonia, where the moderating influence of the Pacific Ocean has little effect because the high Andes mountains act as a barrier. Moving southwards, the land mass narrows, and the Andes lose elevation, so the oceanic influence on climate gets stronger, and may moderate the effects of temperature declines as latitude increases, reducing the advantage for southern birds to excavate north-facing cavities (Berman et al. 2012). In fact, avian populations from islands located south of continental Patagonia (Cape Horn region) show reproductive, foraging, and migratory behaviors that depart from those exhibited by the same species at more northern latitudes, attributed to oceanic influences (Humphrey et al. 1970, Rozzi and Jiménez 2014).

Although we acknowledged the potential weight of this inverse continental effect, we did not include continental effect as part of our Bayesian analyses because it is a complex mix of interacting factors such as temperature, precipitation, cloudiness, atmospheric pressure, and topography; oversimplistic approaches may lead to flawed quantifications (Mikolaskova 2009). Unlike Landler et al.

(2014), we did not have 2 contrasting scenarios to compare the relative effect of continental effects on the orientation of cavity entrances in the Southern Hemisphere. We had hoped to include data from the austral portion of Africa (15°S–34°S) but this region represents a major information gap for cavity-nesting birds (van der Hoek et al. 2017) and we failed to find adequate data for our purposes. In turn, Australia and New Zealand have very few avian excavators. Because of these difficulties and limitations, testing of the effects of macroecological variables as it relates to orientation (and other life-history traits) of Southern Hemisphere avian excavators remains limited.

Preferred Direction(s) of Cavity Entrances Among South American Avian Excavators

Similar to the findings of Landler et al. (2014) for the Northern Hemisphere, cavity-entrance orientation was mostly "nonrandom" in South America. In our model approach, the probability that uniform distributions explained the observed structure of the data was very small (uniform model weight < 30%) in 8 ecoregions, and only the Cerrado and Humid Chaco showed uniformly oriented cavities unequivocally (i.e. with strong model support). But unlike the Northern Hemisphere patterns, unidirectional orientations were not consistent among ecoregions.

Bimodal distributions were most common, either as the top selected model (5 ecoregions) or as a second well-supported alternative (1 ecoregion). Bimodally oriented cavities received the highest model support in the Magellanic Subpolar Forests, while moderate to high support was obtained for top bimodal models in the Dry Chaco and Humid Pampas. Weak support was obtained by bimodal top models in the Atlantic Forest and Valdivian Temperate Rain Forests. In turn, cavity orientation in the Southern Espinal may be either unimodal (top model) or bimodal, based on their almost equal model weights. The widespread bimodality suggests that cavity orientation in South America may be driven by factors beyond latitude, operating at regional or local scales. For example, at our southernmost sites, birds may face a tradeoff between gaining direct solar radiation and avoiding wind. In Patagonia, for example, wind brings rain and snow and may strongly reduce cavity temperatures. Several studies have found that birds orient their nests opposite to the predominant wind direction (Ricklefs and Hainsworth 1969, Conner 1975, Schaefer 1980, Facemire et al. 1990, Norment 1993, Mezquida 2004). From about 36°S (mid-Argentina and Chile) southwards, strong, consistent WNW winds (westerlies) cause a characteristic wind-chill (Paruelo et al. 1998); calm winds seldom occur in austral spring and summer (Beltrán 1997) when most birds breed. Notably, the southernmost ecoregion (Magellanic Subpolar Forests) showed a bimodal cavity orientation that included north and south alternatives. So, even where oceanic influence on climate is at a maximum, a versatile (i.e. bimodal) pattern of cavity orientation may be the best adaptive response to climatic conditions. Interpreting the results for the Valdivian Temperate Rain Forests (the ecoregion with the largest sample size, and second coldest climate), is difficult, as 2 bimodal, 1 unimodal (easterly oriented), and uniform distributions were supported. However, the top, non-axial bimodal model was closely followed by an axial bimodal option, both with very similar mean directions (ϕ1~N and ϕ2~S; see Supplementary Material Appendix S3), also including north and south alternatives. As data were collected from mountainous terrain on both sides of the Andes, topography, wind direction in the valleys, and other local variables may have led to idiosyncratic orientation patterns. On the other hand, the western (Chilean) Andean slopes have high oceanic influence, which is absent on the much harsher eastern (Argentinean) slopes, perhaps leading to heterogeneity in the data.

In the High Monte and Southern Andean Yungas the cavity entrances oriented unimodally to the west, a confusing result in a climatic context. The westerly cavity orientation in these ecoregions seems paradoxical given the intense solar radiation in the afternoon at these low latitude subtropical sites. Wind or other topographic variables may be more important in explaining the patterns in orientation. The northerly dominant orientations in the Northern Espinal also seem weakly advantageous for an extremely dry and warm area, but the support for the top model was moderate (55%), thus more data may be needed to define the orientation patterns in this ecoregion. The Southern Espinal was unimodal (ESE) based on the top model, but a bimodal option (non-axial SSW—NE) had approximately the same weight (differing by mere decimals), as already explained; therefore, uncertainty in the orientation patterns is extremely high for this ecoregion. The Southern Espinal shows the highest inter-seasonal mean temperature variation among the ecoregions analyzed (16°C, Table 1), approaching a "high continentality" class (McBoyle and Steiner 1972). Hence, southerly oriented cavities may be advantageous during the nesting season (spring and summer), when direct solar radiation may accentuate hyperthermic conditions, but likely not for roosting during the winter (mean temperature < 8°C), when northeasterly oriented cavities may be more suitable. Seasonal shifts in the mean orientations of cavities used by woodpecker populations have been documented elsewhere (Inouye et al. 1981, Korol and Hutto 1984, Parks et al. 1996, Lammertink 2011). Information on the nesting habits of avian excavators in the Neotropics is still very preliminary for most species, and much poorer on roosting than nesting habits. Our own data exemplifies this bias: slightly over two thirds of our cavities were located while being used as nests, and the rest were found after construction,

with uncertain use/function. Very infrequently (<10% of all cavities), researchers confirmed a roost function for cavities.

Considering the lack of evidence for large-scale (i.e. continental) patterns of cavity orientation in South America, local factors (micro- and meso-habitat) may play a dominant role in cavity orientation and may differ among and within the ecoregions studied. In forested areas, cavity microclimate may be affected more by forest structure than by cavity orientation. Under vegetation cover, cavity microclimate was relatively independent of orientation in several studies (Maziarz and Wesołowski 2013, van der Hoek 2017). A recent study of the dome-shaped clay nests of the Rufous Hornero (*Furnarius rufus*), which occurs within much of our study area, showed that nests were oriented south (i.e. to avoid excessive heat) only when uncovered (or poorly covered), suggesting that vegetation cover releases the selection of nest orientation from the pressure imposed by solar radiation (Schaaf et al. 2018). Thick and living cavity walls also can buffer temperatures, and social factors, access to foraging areas, and substrate properties may also affect cavity orientation (Jackson and Jackson 2004), but have not been studied in South America.

Evidence suggests that excavators select wood with a specific hardness profile, and such substrates may be in short supply (Schepps et al. 1999, Losin et al. 2006, Matsuoka 2008, Jusino et al. 2015, Lorenz et al. 2015). Where excavators are limited by the availability of suitable nest substrates, cavity orientation may be constrained by the availability of suitably decayed wood, regardless of preferred microclimate. The role of wood hardness in nest-site selection has not been studied in South America and is an important avenue for future research.

Under a multi-model approach, only some South American excavator communities showed clear orientation patterns, while other communities (including ecoregions with large sample sizes) showed moderate to high levels of uncertainty in entrance orientation preferences, with at least two valid options. These overlapping patterns suggest that the circular alignment of cavity entrances, forged as an adaptive response to the environment, may be a more complex aspect of life history than previously considered. In this case, more precise descriptions of the unclear patterns are needed by obtaining additional data considering aspects such as cavity function, seasonal use, etc. Alternatively, disorder in several patterns is also consistent with the idea that cavity entrance orientation is of minor adaptive importance for many South American avian excavators. As the Neotropics hold the highest global richness of tree-excavator species (>130; van der Hoek et al. 2017) of which our study addresses <20%, it is possible that entrance orientation is important in the ecology of some, but not all, austral excavators.

Conclusions and Perspectives

The contrast between our results from the Southern Hemisphere and those from previous work on cavity orientation in the Northern Hemisphere illustrates the importance of including data from both hemispheres when inferring global latitudinal patterns. Our study explores avian nest cavity orientation across several South American ecoregions, and we did not find evidence for consistent latitudinal patterns. Data from additional Southern Hemisphere ecoregions and species might reveal a pattern where cavity entrance orientation is non-random. Future studies should include larger, more balanced samples (regarding species and ecoregions), distinguish between nest and roost cavities, consider seasonality in cavity use, and ideally include direct measurements at local scales, such as substrate availability and cavity microclimate, as well as predictors of cavity temperature (e.g., nest-plant structure; diameter of the trunk at cavity height). These guidelines are applicable worldwide, as many studies from both hemispheres omit these important aspects of avian excavator life history.

We also suggest a revision of the broad-scale patterns of Northern Hemisphere cavity orientations. Our finding that cavity direction showed multimodal distributions in many South American ecoregions suggests that multimodal distributions may be more prevalent than previously acknowledged, and likely occur in many of the studies excluded from Landler et al.'s (2014) meta-analysis of the effects of latitude on cavity orientation. Along with non-unimodal distributional patterns of angular data, higher levels of uncertainty are also likely to arise among Northern Hemisphere avian excavator populations if a multimodal approach is applied, instead of the frequentist-based statistical tests that have been traditionally used with circular biological data (see Fitak and Johnsen 2017). Hypothesis testing, for example, the Hermans-Rasson test, which proved powerful in both unimodal and bimodal situations, can be applied to determine the probability of uniformity (Landler et al. 2019); but if rejected ($P < 0.05$), nothing else is known about the data. An alternative approach that considers a collection of models designed to explore different working hypotheses and selecting the best model in that collection, may reveal subtle, overlooked and parallel/competing patterns in the data, which may alert researchers of alternative drivers of ecological patterns.

Working at a relatively small north–south study area in temperate North America, Butcher et al. (2002) found a significant correlation between the north–south aspect of orientation and the number of hours of direct sunlight received at the nest site, which resulted in an unclear pattern for the overall angular distribution of the cavity data. This example

shows that cavity orientation still may be related to thermoregulatory needs, even where circular distributions do not show unimodal orientations, and that the research on cavity orientation in excavator populations should ideally integrate multiple scales of analysis. In summary, emphasis is needed on directional trends beyond unimodality, better exploratory techniques to describe orientation patterns, and a multiscale approach that attempts to enrich our understanding of cavity orientation by avian excavators.

SUPPLEMENTARY MATERIAL

Supplementary material is available at *Ornithology* online.

ACKNOWLEDGMENTS

We highly appreciate the feedback and assistance from Jolien Cremers and Robert Fitak with the *bpnreg* and *circMLE* packages, respectively. We thank Fabiana Cantarell for assistance with Figure 1. We are grateful to editors and reviewers that provided comments to improve the manuscript, and especially acknowledge the advice from Eric Walters, Lukas Landler, and Wesley Hochachka.

Funding statement: We acknowledge our funding sources and organizations that made this work possible in Supplementary Material Appendix S1.

Ethics statement: All authors minimized the interventions on active nests or roosts by recording the habitat variables with non-destructive techniques when cavities were not in use by animals. Permit numbers are acknowledged in the Supplementary Material Appendix S1.

Author contributions: A.S., N.P., L.R., and V.O. conceived the general idea. V.O. designed the methodology, invited most collaborators, and lead communications. L.C. and S.I. analyzed the data. V.O. led the writing of the manuscript. All authors collected data, contributed critically to drafts, and gave final approval for publication.

Data availability: Analyses reported in this article can be reproduced using the data provided in Supplementary Material Appendix S1 and in Ojeda et al. (2020).

LITERATURE CITED

Akaike, H. (1973). Information theory as an extension of the maximum likelihood principle. In 2nd International Symposium on Information Theory (B. N. Petrov and F. Csaki, Editors). Akademiai Kiado, Budapest, Hungary. pp. 267–281.

Albano, D. (1992). Nesting mortality of Carolina Chickadees breeding in natural cavities. The Condor 94:371–382.

Ardia, D. R., J. H. Pérez, and E. D. Clotfelter (2006). Nest box orientation affects internal temperature and nest site selection by Tree Swallows. Journal of Field Ornithology 77:339–344.

Beltrán, A. (1997). Caracterización microcrimática del Distrito Occidental de la estepa patagónica. MS thesis, FCEyN, Universidad de Buenos Aires, Argentina.

Berman, A. L., G. Silvestri, R. Compagnucci, and V. Velasco Herrera (2012). Oceanic influence on southernmost South American precipitation. Atmósfera 25:217–233.

Burnham, K. P., and D. R. Anderson (2004). Multimodel inference: Understanding AIC and BIC in model selection. Sociological Methods and Research 33:261–304.

Burnham, K. P., D. R. Anderson, and K. P. Huyvaert (2011). AIC model selection and multimodel inference in behavioral ecology: Some background, observations, and comparisons. Behavioral Ecology and Sociobiology 65:23–35.

Burton, N. H. (2006). Nest orientation and hatching success in the Tree Pipit *Anthus trivialis*. Journal of Avian Biology 37:312–317.

Burton, N. H. (2007). Intraspecific latitudinal variation in nest orientation among ground-nesting passerines: A study using published data. The Condor 109:441–446.

Butcher, L. R., S. A. Fleury, and J. M. Reed (2002). Orientation and vertical distribution of Red-naped Sapsucker (*Sphyrapicus nuchalis*) nest cavities. Western North American Naturalist 62:365–369.

Butler, M. W., B. A. Whitman, and A. M. Dufty (2009). Nest box temperature and hatching success of American Kestrels varies with nest box orientation. The Wilson Journal of Ornithology 121:778–782.

Carey, C. (1980). Adaptation of the avian egg to high altitude. American Zoologist 20:449–459.

Carothers, J. H., P. A. Marquet, and F. M. Jaksic (1998). Thermal ecology of a *Liolaemus* lizard assemblage along an Andean altitudinal gradient in Chile. Revista Chilena de Historia Natural 71:39–50.

Conner, R. N. (1975). Orientation of entrances to woodpecker nest cavities. The Auk 92:1371–374.

Cremers, J. (2018). Package: *bpnreg* in R. https://cran.r-project.org/web/packages/bpnreg/bpnreg.pdf.

Cremers, J., and I. Klugkist. (2018). One direction? A tutorial for circular data analysis using R with examples in cognitive psychology. Frontiers in Psychology 9:2040.

Cremers, J., K. T. Mulder, and I. Klugkist. (2018). Circular interpretation of regression coefficients. The British Journal of Mathematical and Statistical Psychology 71:75–95.

Dawson, R. D., C. C. Lawrie, and E. L. O'Brien. (2005). The importance of microclimate variation in determining size, growth and survival of avian offspring: Experimental evidence from a cavity nesting passerine. Oecologia 144:499–507.

Deeming, C. (Editor) (2002). Avian Incubation: Behaviour, Environment and Evolution. Oxford, UK: Oxford University Press.

del Hoyo, J., A. Elliott, J. Sargatal, D. A. Christie, and E. de Juana (Editors) (2018). Handbook of the Birds of the World Alive. Barcelona, Spain: Lynx Edicions. https://www.hbw.com/node/56593.

Derby, R. W., and D. M. Gates (1966). The temperature of tree trunks-calculated and observed. American Journal of Botany 53:580–587.

Dobkin, D. S., A. C. Rich, J. A. Pretare, and W. H. Pyle (1995). Nest-site relationships among cavity-nesting birds of riparian and snowpocket aspen woodlands in the northwestern Great Basin. The Condor 97:694–707.

Dormann, C. F., J. Elith, S. Bacher, C. Buchmann, G. Carl, G. Carré, J. R. García Marquéz, B. Gruber, B. Lafourcade, et al. (2013). Collinearity: A review of methods to deal with it and a simulation study evaluating their performance. Ecography 36:27–46.

Evans, S. W. (2017). The effect of nest site orientation on the breeding success of Blue Swallows *Hirundo atrocaerulea* in South Africa. African Journal of Ecology 56:91–100.

Facemire, C. F., M. E. Facemire, and M. C. Facemire (1990). Wind as a factor in the orientation of entrances of Cactus Wren nests. The Condor 92:1073–1075.

Fitak, R. R., and S. Johnsen. (2017). Bringing the analysis of animal orientation data full circle: Model-based approaches with maximum likelihood. The Journal of Experimental Biology 220:3878–3882.

Gelman, A., J. Hwang, and A. Vehtari (2014). Understanding predictive information criteria for Bayesian models. Statistics and Computing 24:997–1016.

Grueber, C. E., S. Nakagawa, R. J. Laws, and I. G. Jamieson. (2011). Multimodel inference in ecology and evolution: Challenges and solutions. Journal of Evolutionary Biology 24:699–711.

Hansell, M. (2000). Bird Nests and Construction Behaviour. Cambridge, UK: Cambridge University Press.

Hooten, M. B., and N. T. Hobbs (2015). A guide to Bayesian model selection for ecologist. Ecological Monographs 85:3–28.

Humphrey, P. S., D. Bridge, P. W. Reynolds, and R. T. Peterson (1970). Birds of Isla Grande (Tierra del Fuego). Smithsonian Manual (Smithsonian Institution). Lawrence, KS, USA: University of Kansas Museum of Natural History.

Hurvich, C. M., and C. L. Tsai (1989). Regression and time series model selection in small samples. Biometrika 76:297–307.

Idowu, O., O. M. Olarenwaju, and O. Ifedayo (2013). Determination of optimum tilt angles for solar collectors in low-latitude tropical region. International Journal of Energy and Environmental Engineering 4:29.

Inouye, R., N. Huntly, and D. Inouye (1981). Non-random orientation of Gila Woodpecker nest entrances in Saguaro cacti. The Condor 83:88–89.

Jackson, J., and B. J. S. Jackson (2004). Ecological relationships between fungi and woodpecker cavity sites. The Condor 106:37–49.

Jusino, M. A., D. A. Lindner, M. T. Banik, and J. R. Walters (2015). Heart rot hotel: Fungal communities in Red-cockaded Woodpecker excavations. Fungal Ecology 14:33–43.

Korol, J. J., and R. L. Hutto (1984). Factors affecting nest site location in Gila Woodpeckers. The Condor 86:73–78.

Kottek, M., J. Grieser, C. Beck, B. Rudolf, and F. Rubel (2006). World Map of the Köppen-Geiger climate classification updated. Meteorologische Zeitschrift 15:259–263.

Lammertink, M. (2011). Group roosting in the Grey-and-Buff Woodpecker *Hemicircus concretus* involving large numbers of shallow cavities. Forktail 27:78–82.

Landler, L., M. A. Jusino, J. Skelton, and J. R. Walters (2014). Global trends in woodpecker cavity entrance orientation: Latitudinal and continental effects suggest regional climate influence. Acta Ornithologica 49:257–266.

Landler, L., G. D. Ruxton, and E. P. Malkemper. (2019). The Hermans-Rasson test as a powerful alternative to the Rayleigh test for circular statistics in biology. BMC Ecology 19:30.

Lawrence, L. D. (1967). A comparative life-history study of four species of woodpeckers. Ornithological Monographs, no. 5. Washington, D.C., USA: American Ornithologists' Union. pp. 1–156.

Link, W. A., and J. R. Sauer. (2016). Bayesian cross-validation for model evaluation and selection, with application to the North American Breeding Bird Survey. Ecology 97:1746–1758.

Lorenz, T. J., K. T. Vierling, T. R. Johnson, and P. C. Fischer. (2015). The role of wood hardness in limiting nest site selection in avian cavity excavators. Ecological Applications 25:1016–1033.

Losin, N., C. H. Floyd, T. E. Schweitzer, and S. J. Keller (2006). Relationship between Aspen heartwood rot and the location of cavity excavation by a primary cavity-nester, the Red-naped Sapsucker. The Condor 108:706–710.

Lund, U., and C. Agostinelli (2017). Package: *Circular* in R. http://cran.rproject.org/web/packages/circular/circular.pdf.

Mainwaring, M. C., I. Barber, D. C. Deeming, D. A. Pike, E. A. Roznik, and I. R. Hartley. (2017). Climate change and nesting behaviour in vertebrates: A review of the ecological threats and potential for adaptive responses. Biological Reviews of the Cambridge Philosophical Society 92:1991–2002.

Matsuoka, S. (2008). Wood hardness in nest trees of the Great Spotted Woodpecker *Dendrocopos major*. Ornithological Science 7:59–66.

Maziarz, M., and T. Wesołowski (2013). Microclimate of tree cavities used by Great Tits (*Parus major*) in a primeval forest. Avian Biology Research 6:47–56.

McBoyle, G. R., and D. Steiner (1972). A factor analytic approach to the problem of continentality. Geografiska Annaler Series A, Physical Geography 54:12–27.

McCaffrey, J., and C. Galen. (2011). Between a rock and a hard place: Impact of nest selection behavior on the altitudinal range of an alpine ant, *Formica neorufibarbis*. Environmental Entomology 40:534–540.

Mennill, D. J., and L. M. Ratcliffe (2004). Nest cavity orientation in Black-capped Chickadees *Poecile atricapillus*: Do the acoustic properties of cavities influence sound reception in the nest and extra-pair matings? Journal of Avian Biology 35:477–482.

Mezquida, E. T. (2004). Nest site selection and nesting success of five species of passerines in a South American open Prosopis woodland. Journal of Ornithology 145:16–22.

Mikolaskova, K. (2009). Continental and oceanic precipitation régime in Europe. Central European Journal of Geosciences 1:176–182.

Nado, L., and P. Kaňuch (2017). Roost site selection by tree-dwelling bats across biogeographical regions: An updated meta-analysis with meta-regression. Mammal Review 45:215–226.

Norment, C. J. (1993). Nest-site characteristics and nest predation in Harris' Sparrows and White-crowned Sparrows in the Northwest Territories, Canada. The Auk 110:769–777.

Ojeda, V., A. Schaaf, T. A. Altamirano, B. Bonaparte, L. Bragagnolo, L. Chazarreta, K. Cockle, R. Dias, F. Di Sallo, J. T. Ibarra, et al. (2020). Data from: Latitude does not influence cavity entrance orientation of South American avian excavators. Ornithology 138:1–14. doi:10.5061/dryad.0p2ngf1z5.

Olson, D. M., E. Dinerstein, E. D. Wikramanayake, N. D. Burgess, G. V. N. Powell, E. C. Underwood, J. A. D'Amico, I. Itoua, H. E. Strand, J. C. Morrison, et al. (2001). Terrestrial Ecoregions of the World: A new map of life on Earth. BioScience 51:933–938.

Parks, C. G., E. L. Bull, G. Filip, and R. Gilbertson (1996). Wood-decay fungi associated with woodpecker nest cavities in living western larch. Plant Disease 80:959.

Paruelo, J. M., A. Beltrán, E. Jobbagy, O. E. Sala, and R. A. Golluscio (1998). The climate of Patagonia: General patterns and controls on biotic processes. Ecología Austral 8:85–101.

Portet, S. (2020). A primer on model selection using the Akaike Information Criterion. Infectious Disease Modelling 5:111–128.

Prinzinger, R., A. Prebmar, and E. Schleucher (1991). Body temperature in birds. Comparative Biochemistry and Physiology, Part A 99:499–506.

R Core Team (2020). R: A Language and Environment for Statistical Computing. R Foundation for Statistical Computing, Vienna, Austria. https://www.R-project.org.

Remsen, J. V., Jr., J. I. Areta, E. Bonaccorso, S. Claramunt, A. Jaramillo, J. F. Pacheco, M. B. Robbins, F. G. Stiles, D. F. Stotz, and K. J. Zimmer (2020). A Classification of the Bird Species of South America. American Ornithological Society. http://www.museum.lsu.edu/~Remsen/SACCBaseline.htm.

Ricklefs, R., and F. R. Hainsworth (1969). Temperature regulation in nestling Cactus Wrens: Development of homeothermy. The Condor 70:121–127.

Rico, D., and L. Sandoval (2014). Non-random orientation in woodpecker cavity entrances in a tropical rain forest. Ornitología Neotropical 25:1–10.

Rozzi, R., and J. E. Jiménez (Editors) (2014). Sub-Antarctic Magellanic Ornithology. The First Decade of Bird Studies at Omora Ethnobotanical Park, Cape Horn Biosphere Reserve. Denton, TX, USA: University of North Texas Press.

Schaaf, A. A., C. G. García, P. B. Puechagut, L. E. Silvetti, E. Tallei, F. Ortis, and A. Quaglia (2018). Effect of geographical latitude and sun exposure on Rufous Hornero (*Furnarius rufus*) nest orientation. Journal of Ornithology 159:967–974.

Schaefer, V. H. (1980). Geographic variation in the insulative qualities of nests of the Northern Oriole. The Wilson Bulletin 92:466–474.

Schepps, J., S. Lohr, and T. E. Martin (1999). Does tree hardness influence nest-tree selection by primary cavity nesters? The Auk 116:658–665.

Schnute, J. T., and K. Groot (1992). Statistical analysis of animal orientation data. Animal Behavior 43:15–33.

Stevens, A. N. P. (2012). Factors affecting global climate. Nature Education Knowledge 3:18.

Symonds, M. R. E., and A. Moussalli (2011). A brief guide to model selection, multimodel inference and model averaging in behavioural ecology using Akaike's information criterion. Behavioral Ecology and Sociobiology 65:13–21.

van der Hoek, Y. (2017). Southeastern orientation in entrances of Yellow-tufted Woodpecker (*Melanerpes cruentatus*) cavities on the equator. Acta Ornithologica 52:233–238.

van der Hoek, Y., G. V. Gaona, and K. Martin (2017). The diversity, distribution and conservation status of the tree-cavity-nesting birds of the world. Diversity and Distributions 23:1120–1131.

Vehtari, A., A. Gelman, and J. Gabry (2017). Practical Bayesian model evaluation using leave-one-out cross-validation and WAIC. Statistics and Computing 27:1413–1432.

Walsberg, G. E. (1985). Physiological consequences of microhabitat selection. In Habitat Selection in Birds (M. L. Cody, Editor). Academic Press, Orlando, FL, USA. pp. 389–413.

Watanabe, S. (2010). Asymptotic equivalence of Bayes cross validation and widely applicable information criterion in singular learning theory. Journal of Machine Learning Research 11:3571–3594.

Wiebe, K. L. (2001). Microclimate of tree cavity nests: Is it important for reproductive success in Northern Flickers? The Auk 118:412–421.

Zerba, E., and M. L. Morton (1983). Dynamics of incubation in mountain White-crowned Sparrows. The Condor 85:1–11.

Zuur, A. F., E. N. Ieno, N. J. Walker, A. A. Saveliev, and G. M. Smith (2009). Mixed Effects Models and Extensions in Ecology with R. New York, NY, USA: Springer.

Zwartjes, P. W., and S. E. Nordell (1998). Patterns of cavity-entrance orientation by Gilded Flickers (*Colaptes chrysoides*) in cardon cactus. The Auk 115:119–126.

SUPPORTING INFORMATION

Ojeda et al. 2020. Latitude does not influence cavity entrance orientation of South American avian excavators

Appendix S1. Detailed information on the data included in the study. Pages 1–3.

Appendix S2. R Codes: 1) R codes for Bayesian projected normal circular models based on Cremers and Klugkist (2018) and Cremers (2018); 2) R codes for basic circular analysis and model-based approaches with maximum likelihood based on Fitak and Johnsen (2017). Pages 4–6.

Appendix S3. Underlying angular distribution of cavities in 12 South American ecoregions based on probability model selection. Pages 7–19.

Appendix S4. Bayesian projected normal circular mixed-effects models with excavator species as random variable. Pages 20–21.

Appendix S1. Detailed information on the data included in the study.

The "Data set" column refers to a series of data belonging to particular authors. Initials in "Field sites": AR, Argentina; BR, Brazil; CH, Chile. In "Species covered", an * indicates species that were excluded from the Bayesian-projected mixed-effects models due to small sample size (< 9 cavities). Total cavity numbers in the "*n*" column include data from species with small sample sizes, along with cavities not assigned to species (i.e., unknown excavator) that were present in some data sets (also not included in the Bayesian models).

Data set	**Authors**	**Ecoregions**	**Field site(s)** (property, nearby city, national park, country) **(data collection years)**	**Species covered** Taxonomy and nomenclature follow the South American Classification Committee (Remsen et al. 2018).	***n*** Total cavities (included in models)	**Funding (F) and permits (P)**
1	A. Jauregui	• Humid Pampas	• Luis Chico Ranch - Punta Indio, Buenos Aires, AR (2015–2016)	• *Colaptes campestris* • *Colaptes melanochloros* *TOTAL= 2 spp.*	77 (77)	**F**: FONCyT (PICT #2014-3347). **P**: OPDS –DANP (Pcia.de Bs.As.) – Disposición 003/16.
2	A. Wynia J. Jiménez G. Soto P. Vergara	• Magellanic Subpolar Forests	• Omora Park, Navarino Island, CH (2015–2016)	• *Campephilus magellanicus* *TOTAL= 1 sp.*	152 (152)	**F:** Inst. Ecol. & Biodiv. grant ICM P05-002, CONICYT grant PFB-23, FONDECYT 1180978, Partners of the Americas grant, Omora Ethnobotanical Park Found., & Univ. of North Texas. **P**: Based on Chilean law, no permits are required for the type of data used herein.
3	C. Vivanco A. Schaaf L. Rivera N. Politi	• Southern Andean Yungas	• Property of Ledesma Co.- Libertador General San Martin, Jujuy, AR • Parque Nacional Calilegua, Jujuy, AR (2014–2016)	• *Campephilus leucopogon* • *Picumnus cirratus* • *Veniliornis frontalis** • *Colaptes rubiginosus** *TOTAL= 4 spp.* .	145 (103)	**F**: FONCyT (PICT 2012-0892, PICT 2014-1388), CONICET (PIP 112-201201-00259 CO), CONICET-UNJU (PIO 1402014100133), and UNJU (SECTER B 046). Idea Wild, Ass. Field Ornithol, Optic for the Tropics and Rufford Small Grants. **P**: S.M. A. Prov. Jujuy (Res. N 85/2014-DPB) y APN (Proy.DCM 475- 2015).

Part II

4	F. Di Sallo	• Humid Chaco	• Parque Nac. Chaco • Parque Prov. Pampa del Indio. Chaco, AR (2017)	• *Colaptes melanochloros* • *Dryocopus schulzi** • *Campephilus leucopogon* • *Melanerpes cactorum* • *Celeus lugubris** • *Picumnus cirratus* • *Veniliornis mixtus* *TOTAL= 7 spp.*	35 (17)	**F:** Bergstrom Award, Francois Vuilleumier Fund, Idea Wild. **P**: APN permit NEA 418 mod I.
5	F. Lopez L. Bragagnolo M. Santillán	• Southern Espinal	• Reserva Provincial Parque Luro, La Pampa, AR (2012–2017)	• *Veniliornis mixtus* • *Colaptes campestris* • *Colaptes melanochloros* *TOTAL= 3 spp.*	52 (43)	**F**: Proyecto de investigación FCNyE-UNLPam Res. CD 174/13, Grupo aseguradora "La Segunda". **P**: Subs Ecol. & Dirección de Recursos Naturales de la Prov. De La Pampa.
6	M. G. Núñez Montellano	• High Monte	• Cafayate, Salta, AR (2016–2017)	• *Colaptes melanochloros* • *Melanerpes cactorum* *TOTAL= 2 spp.*	40 (40)	**P**: Secretaría de Ambiente, Ministerio de Ambiente y Producción Sustentable, Salta. Expte: 227-207770/15.
7	K. L. Cockle E. B. Bonaparte M. Lammertink	• Atlantic Forests	• PP Cruce Caballero, • San Pedro, • Tobuna, • Reserva de Biosfera Yaboty Misiones, AR (2007–2016)	• *Celeus galeatus* • *Colaptes campestris* • *Colaptes melanochloros* • *Campephilus robustus** • *Dryocopus lineatus* • *Melanerpes flavifrons* • *Veniliornis spilogaster** • *Picumnus temminckii* • *Trogon surrucura* • *Trogon rufus** *TOTAL= 10 spp.*	111 (78)	**F:** Rufford Foundation, Columbus Zoo & Aquarium, Idea Wild, Forest Park Foundation, Cornell Lab of Ornithology, National Geographic, FONCyT (PICT Nº2016-144). **P:** Ministerio de Ecología y RNR (Misiones).
8	L. Rivera N. Politi C. Vivanco A. Schaaf S. Albanesi	• Dry Chaco • Southern Andean Yungas	• Santa Bárbara • Fraile Pintado Jujuy, AR (2009–2010)	• *Campephilus leucopogon* *TOTAL= 1 sp.*	86 (86)	**F:** FONCYT (PICT-2011-1165) **P**: Prov. Jujuy (Res. N 23/2012-DPB).

Part III

9	M. de la Peña	• Dry Chaco • Humid Chaco • Northern Espinal • Parana Flooded Savanna	• Numerous, mainly in Santa Fe province, AR (1970–2016)	• *Campephilus leucopogon* • *Picumnus cirratus* • *Colaptes melanochlroros* • *Colaptes campestris* • *Melanerpes cactorum* • *Melanerpes candidus** • *Veniliornis mixtus* • *Veniliornis passerinus** *TOTAL= 8 spp.*	101 (99)	**P**: not required at time of data collection. No invasive techniques (e.g., manipulation of nest contents) applied.
10	R. Dias	• Cerrado	• Fazenda Água Limpa, Brasília, BR (2007–2014)	• *Campephilus melanoleucos** • *Colaptes campestris* • *Dryocopus lineatus* *TOTAL= 3 spp.*	50 (48)	**F: S**tudent scholarship (Coordenação de Aperfeiçoamento de Pessoal de Nível Superior); François Vuilleumier Fund for Research on Neotropical Birds (NOS); University of Brasília. **P:** 14368 and 2056 (IBAMA).
11	S. Ippi	• Magellanic Subpolar Forests	• Omora Park, Navarino Island, CH (2002–2003)	• *Campephilus magellanicus* *TOTAL= 1 sp.*	14 (14)	**F**: BIOKONCHIL Project (FKZ 01 LM 0208 BMBF); Centro Milenio para Estudios Avanzados en Ecología y Biodiversidad (CMEB, P02-051-FICM). **P**: Based on Chilean law, no permits are required for the type of data used herein.
12	T. Altamirano T. Ibarra	• Valdivian Temperate Rain Forests	• Pucón, La Araucanía, CH (2011–2017)	• *Campephilus magellanicus* • *Pygarrhichas albogularis* • *Colaptes pitius* • *Veniliornis lignarius* *TOTAL= 4 spp.*	130 (128)	**F**: The Peregrine Fund, The Rufford Small Grants for Nature Conservation (14397-2); Francois Vuilleumier Fund for Research on Neotropical Birds (NOS); Idea Wild; NETBIOAMERICAS; CONICYT/ REDES 150047, CONICYT/ FONDECYT de Inicio (11160932); ANID PIA/BASAL FB0002; ANID – Millennium Science Initiative – Center for the Socioeconomic Impact of Environmental Policies, CESIEP Code NCS13_004. **P:** CONAF N° 13/2015 IX and N°03/2018 IX.
13	V. Ojeda L. Chazarreta S. Ippi	• Valdivian Temperate Rain Forests	• Challhuaco Valley-Nahuel Huapi Nat.Park. • Co. Piltriquitrón. Río Negro, AR • Tromen, Lanín Nat. Park Neuquén, AR (1998–2017)	• *Campephilus magellanicus* • *Pygarrhichas albogularis* • *Colaptes pitius* • *Veniliornis lignarius* *TOTAL= 4 spp.*	508 (499)	**F:** UNCo (Sec. Ivest) projects, several from 1998 to 2014 // AAAS/NPS/Canon U.S.A., Inc.: Canon National Parks Science Scholars Program // Idea Wild // FONCyT (PICT 2012-2926) // PIP CONICET Id. #11420110100093. **P**: APN-DRP, #406 (1998) and successive annual renewals.

Appendix S2. R codes.

1) R codes for Bayesian projected normal circular models based on Cremers and Klugkist (2018) and Cremers (2018).

```
library(circular)
library(bpnreg)
library(tibble)
library(dplyr)

datos<-read.csv("Tabla.csv", header = TRUE)
#transform the numeric values of orientation to circular data in degrees
datos$OrientacionGrados <- circular(datos$Orientacion,
                                    units = "degrees",
                                    template = "geographics")
#transform degrees into radians
datos$OrientRads <- datos$OrientacionGrados*pi/180

#center continuous variables at mean = 0
datos$LatC <- datos$Lat - mean(datos$Lat)
datos$AltitudeC <- datos$Altitude - mean(datos$Altitude)
datos$WeightC <- datos$Weight - mean(datos$Weight)

# transforms data to a recognizable dataframe by the package
datos1 <- as.tbl(datos)

#transform the random factors to numeric variable
datos1$WWF <- as.numeric(datos1$WWF)
datos1$BirdSpFinal<- as.numeric(datos1$BirdSpFinal)
# full initial model
```

```
mod_full<-bpnme(pred.I = OrientRads ~ LatC + AltitudeC + WeightC +
          LatC:AltitudeC + LatC:WeightC +
          AltitudeC:WeightC + (1|WWF), data=datos1,
          its = 10000, burn = 1000, n.lag = 3, seed=23)

#to check convergence of the Monte Carlo chains
traceplot(mod_full)

#to calculate the circular coefficients for continuous variables in degrees
coef_circ(mod_full, type <- "continuous")*(180/pi)

#to know the model fit for a Bayesian circular mixed-effects model
fit(mod_full)
```

2) **R codes for basic circular analysis and model-based approaches with maximum likelihood based on Fitak and Johnsen (2017).**

```
# Load libraries
library(circular)
library(CircMLE)

#  Load dataset
data = independent data sets for 1 to 12 (different terrestrial ecoregions).

# Convert to a circular object:
data = as.circular(data, units = 'degrees', template = 'geographics')

# Returns the mean direction of a vector of circular data.
data.mean <-mean.circular(data, na.rm = T)
# Returns the mean resultant length of a vector of circular data (rho)
data.rho<-rho.circular(data, na.rm = T)
# Bootstrap confidence intervals for the parameters of a von Mises distribution: the mean
direction mu, and the concentration parameter kappa.
data.bs <- mle.vonmises.bootstrap.ci(data, reps=10000, alpha = 0.05)
# Basic histogram plot
rose.diag(data, col=" ",  shrink=1.3, units='degrees', template='geographics', axes= F)
# add text (repeat for each cardinal directions)
arctext(x = "N", center = c(0, 0), radius = 1.1, middle = pi/2, cex = 1)

# Add arrow for mean direction and rho length
arrows.circular(mean.circular(data, na.rm = T), y = rho.circular(data, na.rm = T), col = "red",
lwd = 2, lty = 1)
```

```
# Prep data attributed for CircMLE
data = check_data(data)

# Get the circular attributes
params = circularp(data)

# Run CircMLE (default parameters): specifically run four of the ten default models (M1, M2A, M3A, M5A, see de appendix S3for details)
ml.out = circ_mle(data, criterion = "AICc", exclude = c("M2B", "M2C", "M3B", "M4A", "M4B", "M5B"))
# CircMLE output table
model.vector = ml.out$results[1:4, c(2:6, 13, 16, 19)]
# get the parameters from the best fit model
model.vectorBest = ml.out$results[1, 2:6] # results[1:10, 2:6]
q1 = suppressWarnings(as.circular(model.vectorBest[1], control.circular = params))
q2 = suppressWarnings(as.circular(model.vectorBest[4], control.circular = params))
   model.vector = ml.out$results[1, 2:6]

 # Add arrow for mean/s direction/s from the CircMLE output table (repeat for the second mean direction if bimodal)
arrows.circular (q1, col = "black", lwd = 2, lty = 1)
arrows.circular (q2, col = "black", lwd = 2, lty = 1).
```

Literature Cited:

Cremers, J. 2018 [Internet]. Package: *bpnreg* in R. Available at: https://cran.r-project.org/web/packages/bpnreg/bpnreg.pdf.

Cremers J, Klugkist I. 2018. One direction? A tutorial for circular data analysis using R with examples in cognitive psychology. Frontiers in Psychol 9:2040. doi: 10.3389/fpsyg.2018.02040

Fitak RR, Johnsen S. 2017. Bringing the analysis of animal orientation data full circle: model-based approaches with maximum likelihood. J Exper Biol 220:3878–3882.

Appendix S3. Underlying angular distribution of cavities in 12 South American ecoregions based on probability model selection.

Multiple orientation hypotheses were examined simultaneously using the R package *CircMLE* (Fitak and Johnsen 2017) (current v 0.2.3), where models were ranked based on AIC_c. In *CircMLE*, there are 10 maximum separate functions corresponding to the models described by Schnute and Groot (1992). The functions are named to match those of Schnute and Groot (1992) (i.e., M1, M2A, M2B, M2C, M3A, M3B, M4A, M4B, M5A, M5B).

Models fall into these three categories:

(i) a uniform model (**M1**) is that of **random** orientation,
(ii) alternative unimodal models (**M2A, M2B, M2C**) with a **single preferred direction**, and
(iii) alternative bimodal models (**M3, M4, M5**) with **two preferred directions**. The bimodal models further can be **split into axial (M3A, M3B, M4A, M4B**) and **non-axial (M5A, M5B)** types.

As some models are special cases of other models, and considering our aim to describe the main underlying circular structures for cavity orientations, we ran the analyses keeping the models limited to four main types: M1 (uniform), M2A (one direction, i.e., unimodal), M3A (bimodal in opposite directions, i.e., axial), M5A (bimodal in any directions, i.e., non-axial), and compared their likelihoods. Each model is described by up to five parameters: a mean direction ($\boldsymbol{\phi 1}$, in degrees) and concentration parameter ($\boldsymbol{k1}$) for the first mode, a mean direction ($\boldsymbol{\phi 2}$, in degrees) and concentration parameter ($\boldsymbol{k2}$) for the second mode, and the proportional size of the first distribution ($\boldsymbol{\lambda}$; the second distribution is thus fixed at size $1-\lambda$). The *CircMLE* packaged restricted $\boldsymbol{\lambda}$ within bounds $0.25 < \boldsymbol{\lambda} = 0.75$ to minimize the convergence on bimodal distributions with very few cases oriented in one direction, and the rest in another (see Fitak and Johnsen 2017 for further details).

Tables and circular histograms are presented for each ecoregion. In the model tables, AIC_c, ΔAIC_c, and the Akaike weight (w_i) are presented along with the estimated parameters. Models with highest support ($\Delta AIC_c \leq 2$) are in bold, while models with $\Delta AIC_c > 7$ (little support) are in grey.

Circular histograms are shown for the smallest AIC_c model in each ecoregion, where bars represent observed orientation of avian excavator cavities; the estimated mean direction(s) of the top model (black arrows), and the mean direction (μ) of the data (red arrows*)* are also provided. The length of the red arrows corresponds to *rho*, the mean vector length of the circular data (the circle is set to r = 1). White bars were used for uniform top models, light blue for unimodal top models, and grey for bimodal top models. We used the *plotrix* (v 2.2-7) package in R, which has more options for handling plots than the functions of the *Circular* package.

Parameters and confidence intervals (CI) of the von Mises distribution are provided for each ecoregion, below the histograms.

Literature Cited:

Fitak RR, Johnsen S. 2017. Bringing the analysis of animal orientation data full circle: model-based approaches with maximum likelihood. J Exper Biol 220:3878–3882.

Schnute JT, Groot K. 1992. Statistical analysis of animal orientation data. Animal Behav 43:15–33.

Cerrado (*n* = 50)								
Model	**ϕ1**	***k*1**	**λ**	**ϕ2**	***k*2**	**AIC_c**	**ΔAIC_c**	**AIC_c w_i**
M1	**NA**	**0.000**	**1.000**	**NA**	**0.000**	**183.788**	**0.000**	**0.696**
M3A	129	1.073	0.500	310	1.073	186.557	2.769	0.174
M2A	360	0.130	1.000	NA	0.000	187.539	3.752	0.107
M5A	122	1.105	0.457	317	1.105	190.590	6.802	0.024

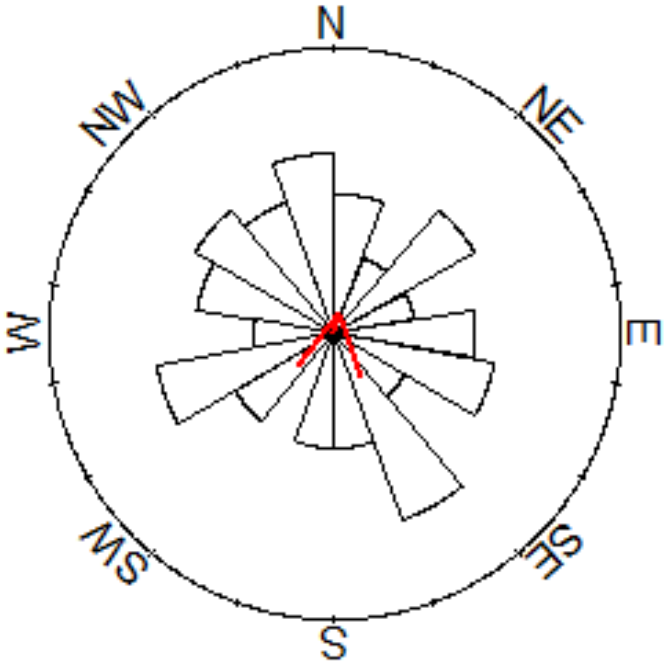

von Mises parameters and CI plot

μ (mean) [CI] = 9 [232 – - 174]

rho = 0.072

κ (*kappa*) [CI] = 0.1447 [0 – - 0.54]

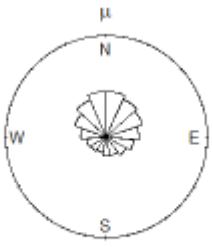

Dry Chaco (*n* = 46)								
Model	**ϕ1**	***k*1**	**Λ**	**ϕ2**	***k*2**	**AIC_c**	**ΔAIC_c**	**AIC_c w_i**
M3A	**56**	**1.698**	**0.500**	**236**	**1.698**	**167.455**	**0.000**	**0.605**
M1	**NA**	**0.000**	**1.000**	**NA**	**0.000**	**169.085**	**1.629**	**0.268**
M5A	231	1.684	0.442	57	1.684	171.648	4.193	0.074
M2A	71	0.213	1.000	NA	0.000	172.325	4.870	0.053

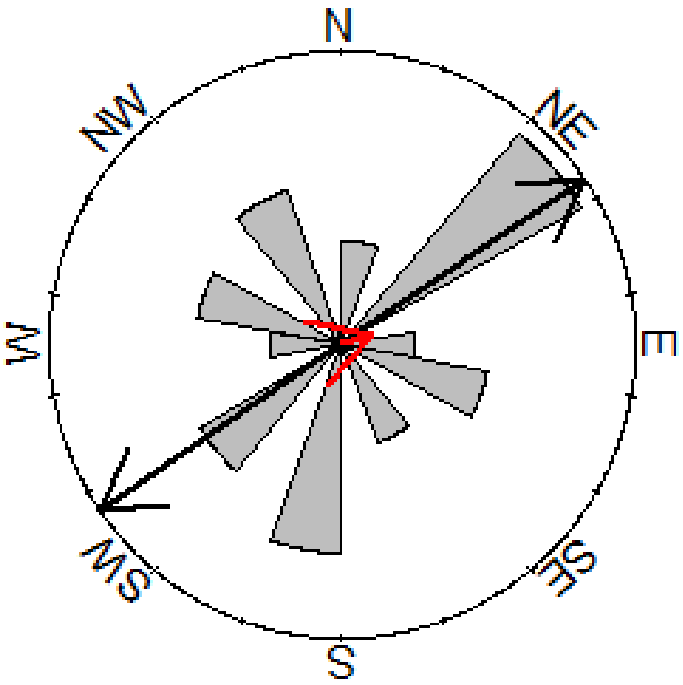

von Mises parameters and CI plot

μ (mean) [CI] = 71 [328 – 266]

rho = 0.106

κ (*kappa*) [CI] = 0.2134 [0 – 0.69]

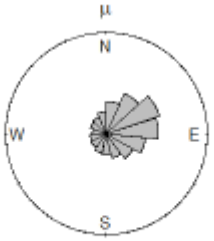

Southern Andean Yungas (*n* = 186)								
Model	**ϕ1**	***k*1**	**Λ**	**ϕ2**	***k*2**	**AIC_c**	**ΔAIC_c**	**AIC_c w_i**
M2A	**267**	**0.263**	**1.00**	**NA**	**0.000**	**681.397**	**0.000**	**0.609**
M1	NA	0.000	1.00	NA	0.000	683.690	2.293	0.194
M5A	277	0.765	0.68	110	0.765	684.242	2.845	0.147
M3A	101	0.721	0.50	281	0.721	686.406	5.009	0.050

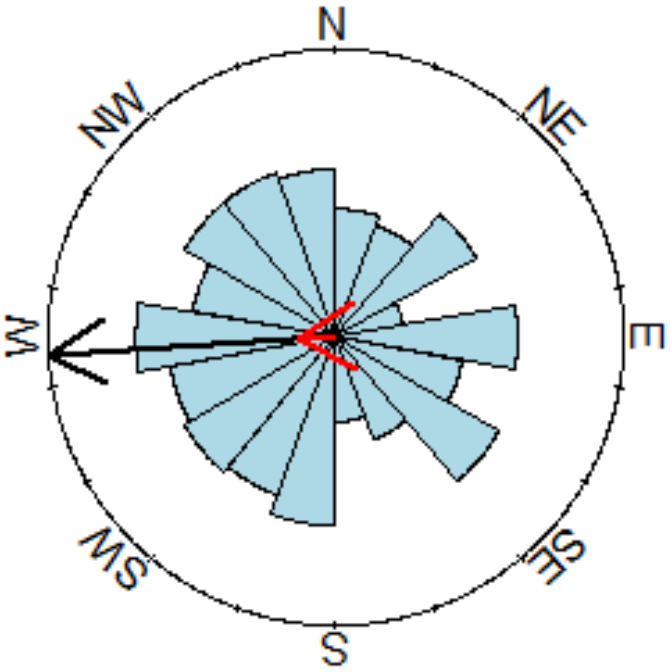

von Mises parameters and CI plot

μ (mean) [CI] = 266 [213 – 317]

rho = 0.130

κ (*kappa*) [CI] = 0.263 [0.06 – 0.48]

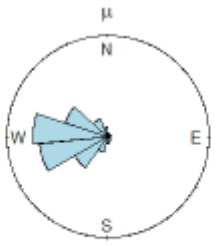

Atlantic Forest (*n* = 113)								
Model	**ϕ1**	***k*1**	**λ**	**ϕ2**	***k*2**	**AIC_c**	**ΔAIC_c**	**AIC_c w_i**
M3A	**154**	**1.150**	**0.500**	**334**	**1.150**	**415.166**	**0.000**	**0.420**
M1	**NA**	**0.000**	**1.000**	**NA**	**0.000**	**415.360**	**0.194**	**0.381**
M2A	175	0.160	1.000	NA	0.000	418.025	2.859	0.100
M5A	331	1.162	0.424	158	1.162	418.054	2.888	0.099

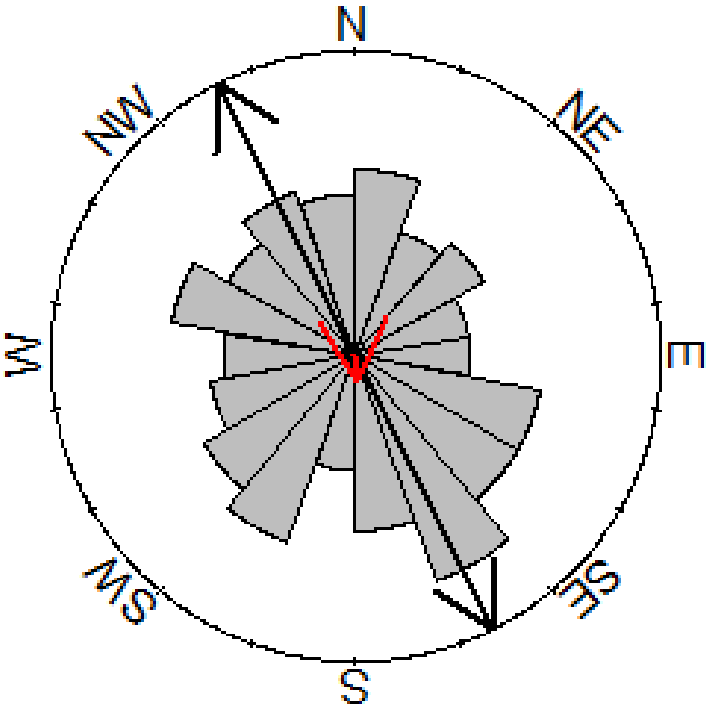

von Mises parameters and CI plot

μ (mean) [CI] = 175 [59 – 317]

rho = 0.08

κ (*kappa*) [CI] = 0.1602 [0.0 – 0.44]

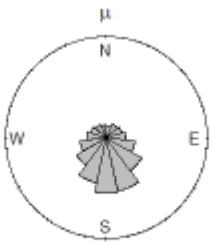

High Monte (*n* = 40)								
Model	**ϕ1**	***k*1**	**λ**	**ϕ2**	***k*2**	**AIC_c**	**ΔAIC_c**	**AIC_c w_i**
M2A	**263**	**1.049**	**1.000**	**NA**	**0.000**	**133.129**	**0.000**	**0.845**
M5A	246	1.651	0.749	5	1.651	136.581	3.452	0.151
M1	NA	0.000	1.000	NA	0.000	147.030	13.901	0.001
M3A	240	1.306	0.500	60	1.306	149.212	16.083	0.000

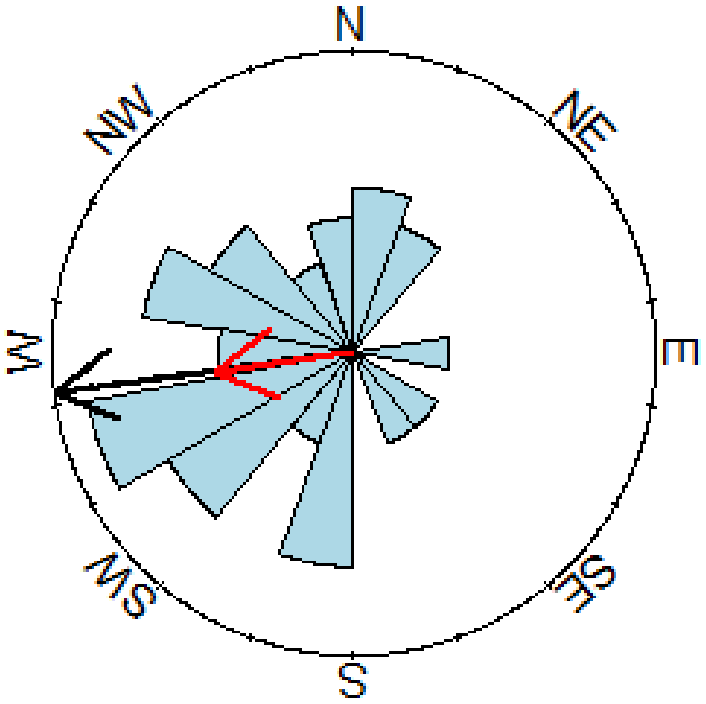

von Mises parameters and CI plot

μ (mean) [CI] = 263 [238 – 290]

rho = 0.463

κ (*kappa*) [CI] = 1.044 [0.58 – 1.67]

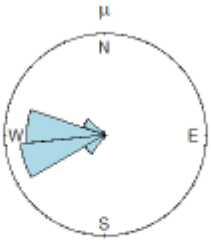

Humid Chaco (*n* = 46)								
Model	**ϕ1**	***k*1**	**λ**	**ϕ2**	***k*2**	**AIC_c**	**ΔAIC_c**	**AIC_c w_i**
M1	**NA**	**0.000**	**1.000**	**NA**	**0.000**	169.085	**0.000**	**0.844**
M3A	199	0.927	0.500	19	0.927	172.512	3.428	0.132
M2A	0	0.158	1.000	NA	0.000	172.733	3.649	0.118
M5A	209	0.944	0.426	12	0.944	176.473	7.388	0.018

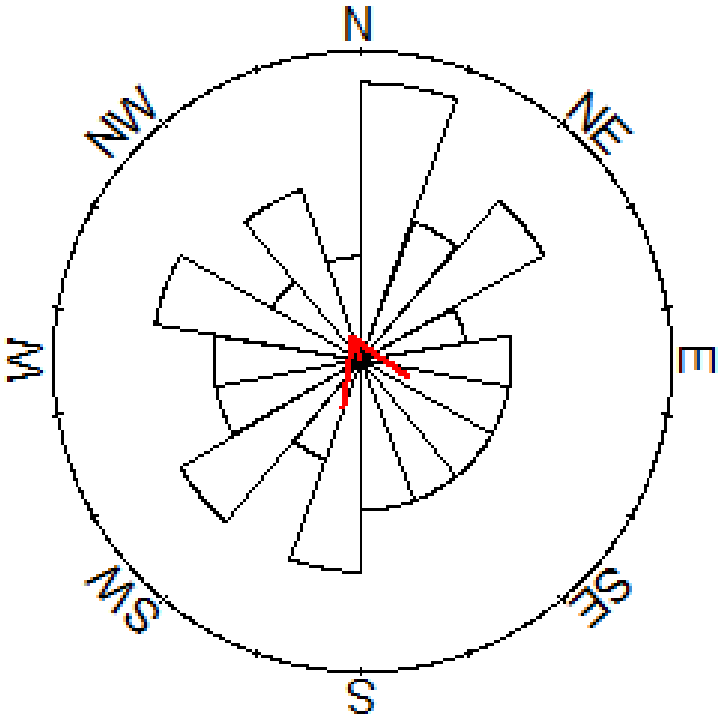

von Mises parameters and CI plot

μ (mean) [CI] = 336 [190 – 125]

rho = 0.0905

κ (*kappa*) [CI] = 0.1819 [0.0 – 0.62]

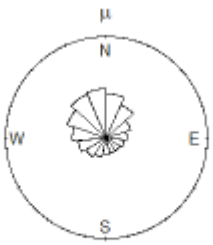

Parana Flooded Savanna (*n* = 9)								
Model	**ϕ1**	***k*1**	**λ**	**ϕ2**	***k*2**	**AIC_c**	**ΔAIC_c**	**AIC_c w_i**
M1	**NA**	**0.000**	**1.000**	**NA**	**0.000**	**33.082**	**0.000**	**0.491**
M2A	**316**	**1.321**	**1.000**	**NA**	**0.000**	**33.165**	**0.083**	**0.471**
M3A	304	1.554	0.500	124	1.554	38.281	5.200	0.036
M5A	301	1.651	0.749	51	1.651	45.214	12.133	0.001

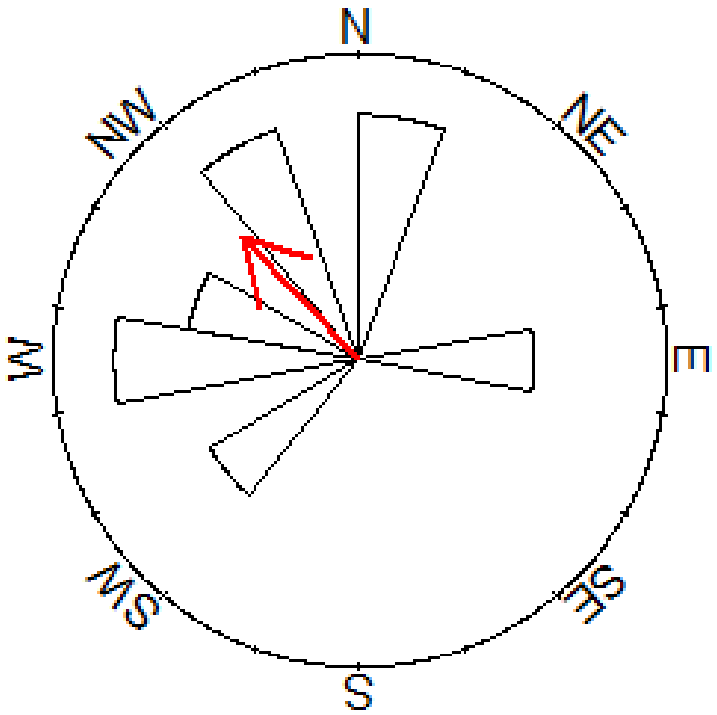

von Mises parameters and CI pl

μ (mean) [CI] = 316 [274 – 9]

rho = 0.549

κ (*kappa*) [CI] = 1.316 [0.3 – 3.4]

Northern Espinal (*n* = 78)								
Model	**ϕ1**	***k*1**	**λ**	**ϕ2**	***k*2**	**AIC_c**	**ΔAIC_c**	**AIC_c w_i**
M2A	**352**	**0.403**	**1.000**	**NA**	**0.000**	**284.727**	**0.000**	**0.554**
M1	**NA**	**0.000**	**1.000**	**NA**	**0.000**	**286.709**	**1.981**	**0.206**
M5A	125	1.267	0.325	329	1.267	286.859	2.132	0.191
M3A	139	1.041	0.500	319	1.041	289.539	4.811	0.050

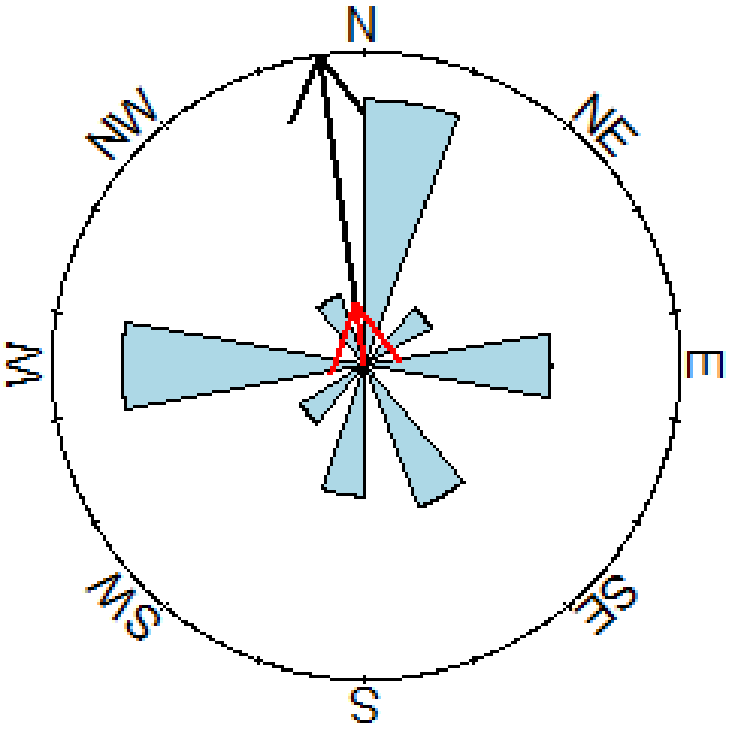

von Mises parameters and CI plot

μ (mean) [CI] = 351 [303 – 46]

rho = 0.197

κ (*kappa*) [CI] = 0.4028 [0.09 – 0.75]

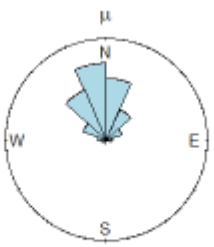

Humid Pampas (*n* = 77)								
Model	**ϕ1**	***k*1**	**λ**	**ϕ2**	***k*2**	**AIC_c**	**ΔAIC_c**	**AIC_c w_i**
M3A	**178**	**1.497**	**0.500**	**358**	**1.497**	**280.767**	**0.000**	**0.604**
M1	NA	0.000	1.000	NA	0.000	283.033	2.266	0.194
M5A	173	1.533	0.551	360	1.533	283.772	3.005	0.134
M2A	146	0.229	1.000	NA	0.000	285.190	4.423	0.066

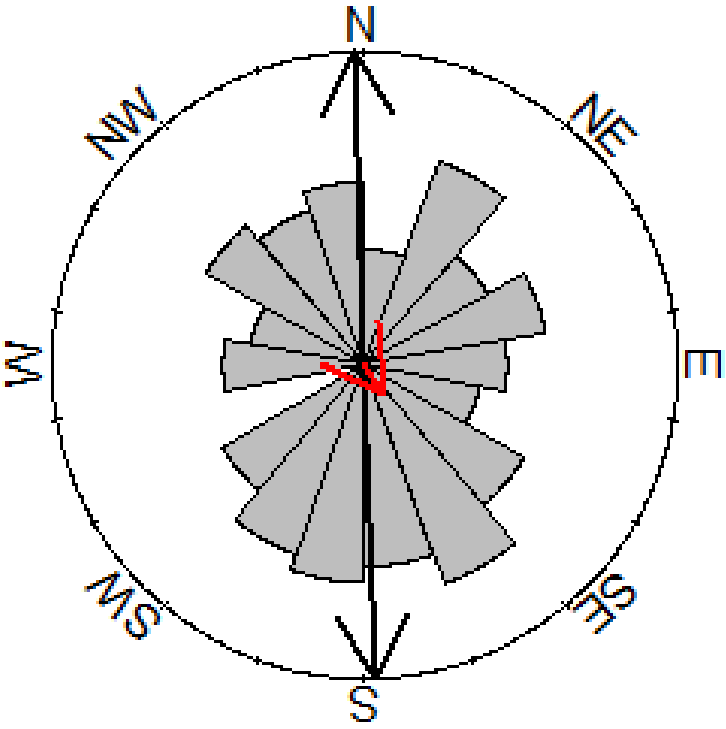

von Mises parameters and CI plot

μ (mean) [CI] = 146 [243 – 22]

rho = 0.114

κ (*kappa*) [CI] = 0.2293 [0.0 – 0.56]

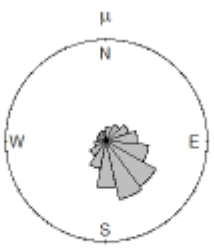

Southern Espinal (*n* = 52)								
Model	**ϕ1**	***k*1**	**λ**	**ϕ2**	***k*2**	**AIC_c**	**ΔAIC_c**	**AIC_c w_i**
M2A	**111**	**0.469**	**1.000**	**NA**	**0.000**	**189.887**	**0.000**	**0.345**
M5A	**59**	**1.617**	**0.556**	**198**	**1.617**	**189.909**	**0.022**	**0.342**
M1	**NA**	**0.000**	**1.000**	**NA**	**0.000**	**191.139**	**1.252**	**0.185**
M3A	**39**	**1.357**	**0.500**	**219**	**1.357**	**191.873**	**1.986**	**0.128**

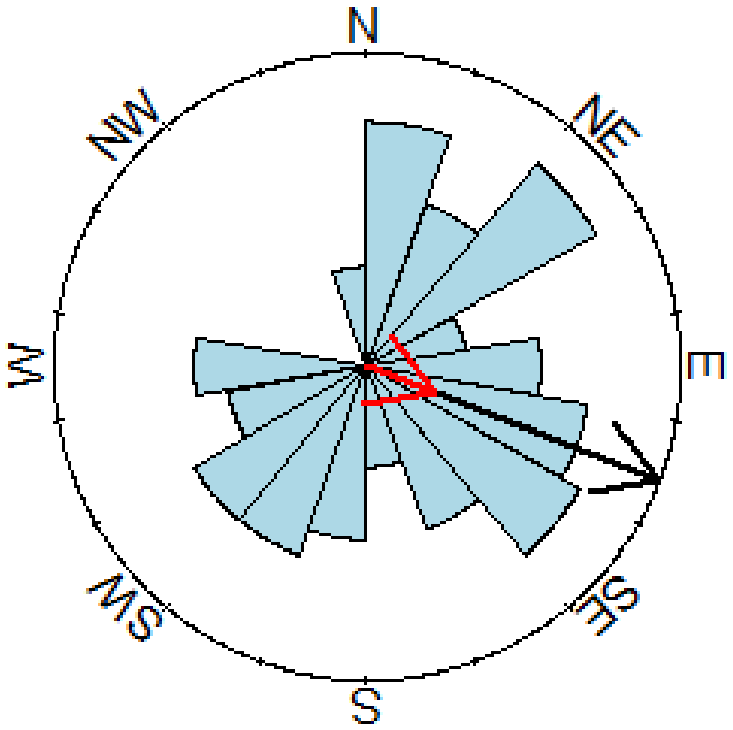

von Mises parameters and CI plot

μ (mean) [CI] = 111 [63 – 167]

rho = 0.228

κ (*kappa*) [CI] = 0.4692 [0.11 – 0.84]

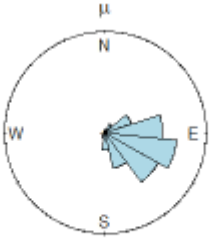

Valdivian Temperate Rain Forests (*n* = 638)								
Model	**ϕ1**	***k*1**	**λ**	**ϕ2**	***k*2**	**AIC_c**	**ΔAIC_c**	**AIC_c w_i**
M5A	**180**	**0.758**	**0.473**	**19**	**0.758**	**2343.350**	**0.000**	**0.381**
M3A	**190**	**0.736**	**0.500**	**10**	**0.736**	**2344.299**	**0.949**	**0.237**
M2A	**82**	**0.122**	**1.000**	**NA**	**0.000**	**2344.413**	**1.063**	**0.224**
M1	**NA**	**0.000**	**1.000**	**NA**	**0.000**	**2345.131**	**1.781**	**0.157**

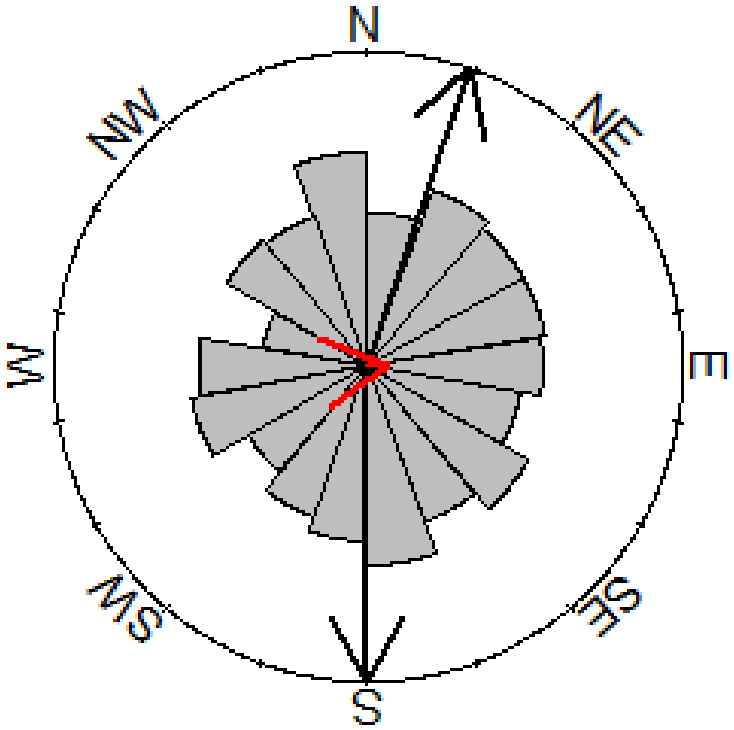

von Mises parameters and CI plot

μ (mean) [CI] = 82 [23 – 142]

rho = 0.061

κ (*kappa*) [CI] = 0.122 [0.02 – 0.23]

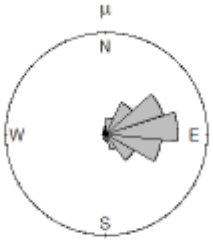

Magellanic Subpolar Forests (*n* = 166)								
Model	**ϕ1**	***k*1**	**Λ**	**ϕ2**	***k*2**	**AIC_c**	**ΔAIC_c**	**AIC_c w_i**
M5A	**327**	**1.480**	**0.570**	**120**	**1.480**	**598.006**	**0.000**	**0.922**
M3A	135	1.362	0.500	315	1.362	603.533	5.527	0.058
M2A	15	0.319	1.000	NA	0.000	605.952	7.946	0.017
M1	NA	0.000	1.000	NA	0.000	610.175	12.169	0.002

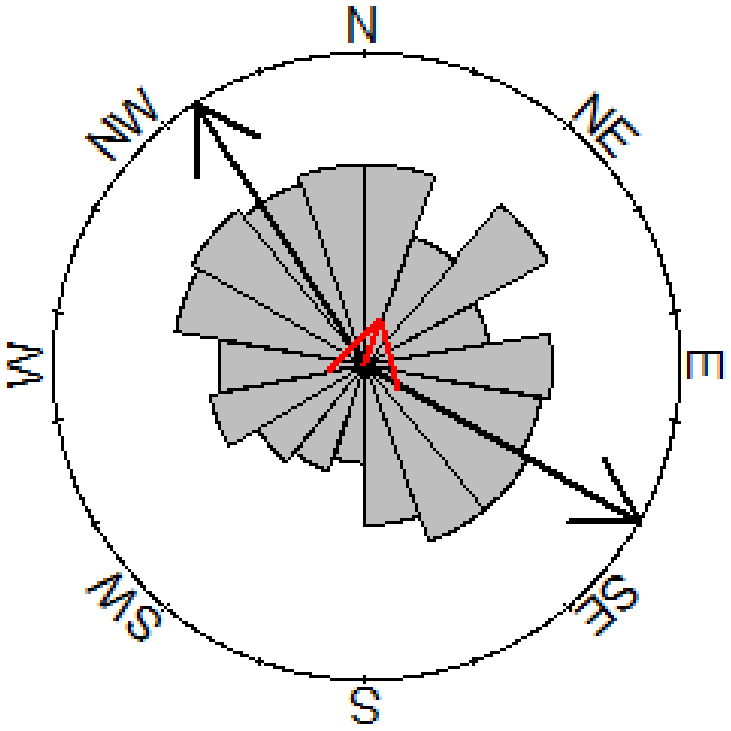

von Mises parameters and CI plo

μ (mean) [CI] = 15 [336 – 62]

rho = 0.158

κ (*kappa*) [CI] = 0.3192 [0.11 – 0.53]

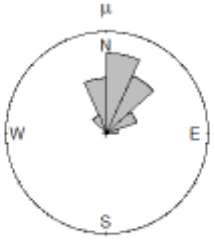

Appendix S4. Bayesian projected normal circular mixed-effects models with excavator species as random variable.

These models test for the effects of latitude, elevation, species mean weight, and the interactions between latitude and the other two explanatory variables, on cavity orientation of South American avian excavators, where excavator species is a random factor. Models are ordered from lowest to highest Watanabe-Akaike information criterion (WAIC, Watanabe 2010). The log pointwise predictive density (lppd, the log-likelihood evaluated at the posterior simulations of the parameter values) and the effective number of parameters (pD, a measure of model complexity computed according to Gelman et al. (2014)) are provided (Hooten and Hobbs 2015, Vehtari et al. 2017).

Model	lppd	pD	WAIC	ΔWAIC
Latitude	-2528.16	10.48	5077.30	0.00
Null model	-2529.11	9.57	5077.38	0.08
Latitude + Elevation + Weight + Latitude x Elevation	-2522.59	16.15	5077.49	0.19
Latitude + Weight + Latitude x Weight	-2528.54	10.22	5077.50	0.20
Latitude + Elevation + Latitude x Elevation	-2524.34	14.49	5077.66	0.36
Latitude + Weight	-2526.55	12.50	5078.10	0.80
Latitude + Elevation + Weight + Latitude x Weight	-2527.39	11.92	5078.61	1.31
Latitude + Elevation + Weight	-2525.56	14.47	5080.06	2.76
Latitude + Elevation	-2527.37	12.69	5080.10	2.80
Latitude + Elevation + Weight + Latitude x Elevation + Latitude x Weight	-2525.72	15.04	5081.52	4.22

Posterior modes of the circular regression coefficients for the variables included in the lowest WAIC model with excavator species as random factor (see previous Table). References: b_c is the slope of the circular regression line at the inflection point, SAM is the slope of the circular regression line at the average of the predictor, and AS is the average slope over all values of the each predictor variable. LB HPD and UB HPD indicate the lowest and the upper bounds of the highest posterior density interval of the coefficients, respectively (Cremers and Klugkist 2018).

		Mode	**LB HPD**	**UB HPD**
Latitude	b_c	9.45	-230.11	288.81
	SAM	20.35	-120.54	139.72
	AS	0.21	-69.94	64.86

Literature Cited:

Cremers J, Klugkist I. 2018. One direction? A tutorial for circular data analysis using R with examples in cognitive psychology. Frontiers in Psychology 9:2040. doi: 10.3389/fpsyg.2018.02040

Gelman A, Hwang J, Vehtari A. 2014. Understanding predictive information criteria for Bayesian models. Stat Comput 24:997–1016.

Hooten MB, Hobbs, NT. 2015. A guide to Bayesian model selection for ecologist. Ecol Monog 85:3–28.

Vehtari A, Gelman A, Gabry J. 2017. Practical Bayesian model evaluation using leave-one-out cross-validation and WAIC. Statistics and Computing 27:1413–1432.

Watanabe S. 2010. Asymptotic equivalence of Bayes cross validation and widely applicable information criterion in singular learning theory. J Mach Learn Res 11:3571–3594.